Showcasing the review on electrochemical energy storage with carbon onions by the INM – Leibniz Institute for New Materials (Prof. Presser, M. Zeiger, N. Jäckel), Germany, and Prof. Mochalin (Missouri University of Science and Technology), USA.

Title: Review: carbon onions for electrochemical energy storage

Carbon onions are nanoscopic carbon spheres with tunable structure. The combination of highly accessible outer surface, high interparticle pore volume and high electrical conductivity has made carbon onions highly attractive for electrochemical applications. In particular, ultrafast supercapacitors, high performance pseudocapacitors, improved conductive additives for batteries and supercapacitors, and redox hybrids are being reviewed.

As featured in:

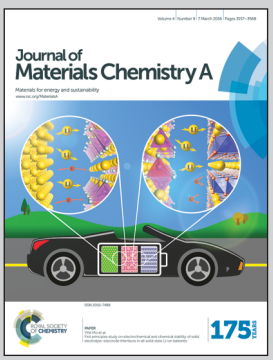

See Vadym N. Mochalin, Volker Presser *et al.*, *J. Mater. Chem. A*, 2016, **4**, 3172.

ROYAL SOCIETY OF CHEMISTRY

www.rsc.org/MaterialsA

Registered charity number: 207890

Journal of Materials Chemistry A

REVIEW

View Article Online
View Journal | View Issue

Cite this: J. Mater. Chem. A, 2016, 4, 3172

Review: carbon onions for electrochemical energy storage

Marco Zeiger,[ab] Nicolas Jäckel,[ab] Vadym N. Mochalin*[c] and Volker Presser*[ab]

Carbon onions are a relatively new member of the carbon nanomaterials family. They consist of multiple concentric fullerene-like carbon shells which are highly defective and disordered. Due to their small size of typically below 10 nm, the large external surface area, and high conductivity they are used for supercapacitor applications. As electrode materials, carbon onions provide fast charge/discharge rates resulting in high specific power but present comparatively low specific energy. They improve the performance of activated carbon electrodes as conductive additives and show suitable properties as substrates for redox-active materials. This review provides a critical discussion of the electrochemical properties of different types of carbon onions as electrode materials. It also compares the general advantages and disadvantages of different carbon onion synthesis methods. The physical and chemical properties of carbon onions, in particular nanodiamond-derived carbon onions, are described with emphasis on those parameters especially important for electrochemical energy storage systems, including the structure, conductivity, and porosity. Although the primary focus of current research is on electrode materials for supercapacitors, the use of carbon onions as conductive additives and for redox-active species is also discussed.

Received 15th October 2015
Accepted 7th December 2015

DOI: 10.1039/c5ta08295a

www.rsc.org/MaterialsA

1. Introduction

1.1 Electrochemical energy storage with nanocarbons

Carbon materials have always been at the focal point of energy applications, ranging from the ongoing use of coal as the primary energy source to the utilization as the standard anode material for lithium ion batteries. The emergence of new carbon nanoforms, foremost carbon nanotubes and graphene, has

[a]INM – Leibniz Institute for New Materials, 66123 Saarbrücken, Germany. E-mail: volker.presser@leibniz-inm.de
[b]Department of Materials Science and Engineering, Saarland University, 66123 Saarbrücken, Germany
[c]Missouri University of Science & Technology, Rolla, MO 65409, USA. E-mail: mochalinv@mst.edu

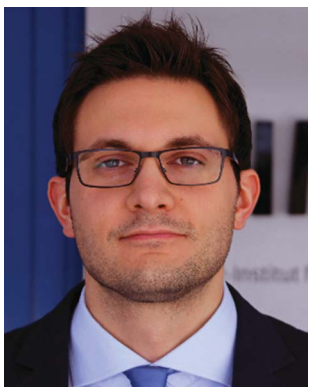

Marco Zeiger studied Microfabrication and Nanostructures in the Department of Physics and Mechatronics at Saarland University, Germany. Between 2011 and 2013 he worked in the Metallic Microstructures Group of the INM – Leibniz Institute for New Material on the antibacterial properties of copper and its application in touch surfaces. In 2013 he joined the INM Energy Materials Group working on the synthesis and characterization of nanodiamonds and carbon onions with the focus on electrochemical energy storage. Receiving his M.Sc., he began his PhD studies in 2014 on the development of carbon/metal oxide hybrid materials for redox-enabled energy storage devices.

Nicolas Jäckel studied Microfabrication and Nanostructures in the Department of Physics and Mechatronics at Saarland University, Germany. In 2012 he completed his Bachelors thesis on gas sensors at Drägerwerk AG & Co. KGaA, Lübeck. In 2013, he joined the INM Energy Materials Group working on atomic layer deposition and advanced supercapacitors. In 2015 he received his M.Sc. and started his PhD studies. In collaboration with the Group of Prof. Doron Aurbach, Bar-Ilan University, Israel, he is working on the in situ electrochemical methodology for tracking of charging and related mechanical processes in batteries and supercapacitors.

propelled research related to electrochemical energy storage and conversion, leading to what has been coined the "carbon new age".[1] Among all carbon nanoforms and allotropes, carbon onions are one of the most interesting. Carbon onions, also called onion-like carbon or carbon nano-onions, are nanoscopic carbon particles, with a nearly spherical shape made of multiple enclosed fullerene-like carbon shells. The unique combination of high electrical conductivity (comparable to carbon black), large external surface area, and nanoscopic size (commonly below 10 nm), alongside the possibility for large-scale synthesis and chemical modification,[2] has made this material very attractive for applications, ranging from lubrication and catalysis[3] to electrochemical energy storage (EES),[4] biomedical imaging,[2] and water treatment.[5] Carbon onions have been explored intensively for EES applications as electrode materials for ultrafast charge/discharge devices[6] or as a potent conductive additive to enhance the power handling ability of activated carbon.[7] With the increasing number of carbon onion studies for advanced electrochemical applications,[8,9] this review summarizes the state-of-the-art and provides a comprehensive overview of relevant topics of the structure as well as electrochemical and relevant properties of carbon onions.

Efficient and adaptable energy storage has emerged as a key enabling technology for the large scale utilization of renewable energy from sustainable ("green") sources, such as solar or wind power.[10,11] Carbon nanomaterials and hybrids have been at the focal point of many electrochemical energy storage technologies,[12,13] as exemplified by supercapacitors[14] or batteries.[15,16] The electrochemical energy storage mechanisms range from ion electrosorption and interfacial redox-reactions of the electrode material or bulk faradaic reactions of the electrolyte to ion intercalation into the anode or cathode.[12,17,18] The most prominent group of supercapacitors, the electrical double-layer capacitors (EDLCs), capitalizes on fast ion electrosorption to enable very high power handling.[14] Energy is stored at the electrode/electrolyte interface where electric charges are accumulated on the electrode surfaces and ions of opposite charge are arranged on the electrolyte side of both electrodes. A high electrosorption rate and the absence of (electro)chemical reactions (faradaic reactions) enable very high specific power of EDLCs at the cost of a rather low specific energy compared to batteries.[19] An approximate storage capacity for pure ion electrosorption is $\sim$0.1 F m^{-2} = 0.03 mA h m^{-2} at 1 V, when normalized to the surface area of a nanoporous carbon electrode.[20]

Considering the limitations of ion electrosorption in stored energy, it is intriguing to utilize faradaic reactions to enhance the energy storage capacity.[21] This can be achieved by adding redox-active materials, such as electroactive polymers, surface functional groups, transition metal oxides, or by using a redox-active electrolyte, such as the iodine/iodide redox couple.[17] Depending on the electrochemical response, the resulting behavior may be classified as capacitor-like (pseudocapacitor) or battery-like (sometimes referred to as the supercabattery).[18,22] Operation of such hybrid cells, in contrast to EDLCs, involves the charge transfer between the electrode and electrolyte where, for example, ruthenium changes its oxidation state from Ru(III) to Ru(VI).[23–26] Carbon onions, featuring a fully available outer surface, are a highly attractive material for hybrid designs because of the facile access to the surface and the ease of functionalization with, for example, metal oxides or surface groups, to enable enhanced energy storage capacity.[27] For a more substantial review of the energy storage technologies, such as supercapacitors, batteries, and hybrid devices, the reader is referred to recent comprehensive articles on these topics.[14,18,28]

1.2 What is a carbon onion?

Carbon onions can be defined by virtue of their structure as spherical or polyhedral carbon nanoparticles, often smaller

Vadym N. Mochalin received his PhD in Physical Chemistry from L. M. Litvinenko Institute of Physical Organic and Coal Chemistry, National Academy of Sciences of Ukraine, and M.S. in Biochemistry from Donetsk National University, Ukraine. In 2005–2015 he worked with Prof. Yury Gogotsi at Drexel University, leading the research on nanodiamonds. He is now Associate Professor in Chemistry at Missouri University of Science and Technology. His current research interests include synthesis, characterization, purification, chemical modification, computational modeling, and applications of nanodiamonds, MXene, nanoonions, nanocarbons, and other materials for composites, energy storage, biomedical applications, and extreme environments.

Volker Presser obtained his PhD in Applied Mineralogy in 2006 from the Eberhard Karls University in Tübingen, Germany. As a Humboldt Research Fellow and Research Assistant Professor, he worked between 2010 and 2012 at the A.J. Drexel Nanotechnology Institute in the team of Yury Gogotsi at Drexel University, Philadelphia, USA. As Chair for Energy Materials, he is Full Professor at the Department of Materials Science and Engineering at Saarland University and Group Leader at the INM – Leibniz Institute for New Materials in Saarbrücken, Germany. His research activities include nanocarbon and hybrid nanomaterials for electrochemical energy storage, harvesting, and water desalination.

than 10 nm, consisting of several fullerene-like carbon shells enclosed in a "Russian doll" manner which are defective and disordered to a certain degree.[29] This distinct multi-layer architecture is also the name-giving feature for carbon onions. First discovered by Iijima in 1980 and described by Ugarte in 1992,[30,31] carbon onions are a rather novel addition to the carbon materials family. Depending on their synthesis method and the synthesis parameters, the resulting carbon onions differ in size, chemical composition, phase, and morphology. The most commonly used synthesis method for carbon onions is graphitization of nanodiamonds at high temperatures (>1700 °C) in an inert gas or vacuum. The resulting carbon onions are typically smaller than 10 nm and present a high degree of carbon ordering. The amount of non-carbon material is very small (typically in the range of 1–2 mass%) and surface areas can reach up to 600 $m^2\ g^{-1}$. Key structural characteristics of a carbon onion are summarized in Fig. 1, with more details about the synthesis methods given in the next section.[32]

1.3 Nomenclature

So far, there is no consistent nomenclature for carbon onions in the literature. Consistent nomenclature is a notorious issue throughout the entire field of nanocarbons, especially when it comes to rather new carbon structures.[33] Most reports, often interchangeably, use either "carbon onions", "carbon nano-onions", or "onion-like carbon". All three are not in agreement with the nomenclature for sp^2-hybridized carbon nanoforms by Suarez-Martinez, Grobert, and Ewels.[29] They suggest consistently calling carbons with an "onion" structure "multi-wall fullerene". This unifying nomenclature employs purely geometrical classification, independent of the state of carbon ordering (defects), particle size and shape, or synthesis method. When considering very large structures referred to as carbon onions with size more than 100 nm and a high defect density, the conceptual description as "fullerene", normally applied to molecules, may be arguable. On the other hand, onion-like carbon, which is an umbrella term for any onion-type structure is just as vague as other terms, like diamond-like carbon. Also, compared to carbon nanotubes, the differentiation between single-, double-, few-, and multi-wall architectures is not practical for carbon onions: almost all carbon onions qualify as multi-wall structures. Subtler differentiation in the name based on the shape ranging from spherical to polyhedral is also neither practical nor easily quantifiable. Based on considerations similar to those used in the nomenclature of carbon nanotubes, we suggest application of the term "carbon onions" only to those carbon particles that have at least 4 shells (like multi-wall carbon nanotubes), a size smaller than 100 nm, spherical or polyhedral shape, and a partially defective structure (amorphous domains, or islands of sp^3-hybridized carbon). The distinct structural characteristic defining carbon onions should be the clearly visible multi-shell character. This nomenclature also includes hollow carbon onions (hollow core), and carbon onions with a core (*e.g.*, metal clusters or residual nanodiamonds remaining inside the carbon onion due to incomplete transformation).

As with any other material, the issues related to nomenclature for carbon onions are much more difficult to address than in the nomenclature of molecules. The key reason for this, as the authors believe, is the undefined variable composition of a material, whereas the composition of molecules, by definition, is always fixed. Taking into consideration chemical modifications of materials, any attempts to use nomenclature in the sense it is applied to molecules, become meaningless. This necessitates alternative approaches to distinguish materials. A more practical differentiation is based on the type of precursor and/or the synthesis method. For example, clearly stating "nanodiamond-derived carbon onions" *versus* "arc-discharge carbon onions" unambiguously refers to a specific group of carbons.

Finally, the community may consider to adopt a size-dependent differentiation between carbon onions (in general) and carbon nano-onions, with the latter referring to carbon onions smaller than 10 nm. This suggestion is motivated by the differentiation between nanodiamonds and single-digit nanodiamonds, with the latter covering the range below 10 nm.[34] Yet, it is beyond the scope of this review to establish a clear nomenclature recommendation. Thus, in the absence of definite nomenclature, thorough and complete description of the

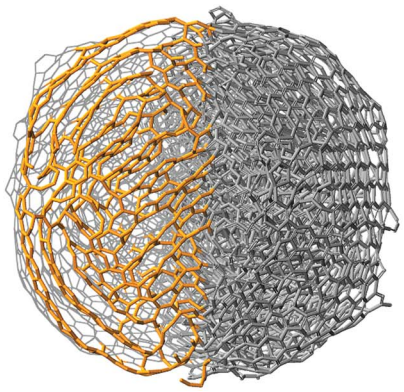

Fig. 1 Typical features of carbon onions.

experimental procedure and the obtained carbon onion structures becomes even more important to enable a scientifically useful basis for comparison.

2. Synthesis of carbon onions

2.1 Overview of synthesis methods

Different methods can be used for the synthesis of carbon onions, such as decomposition of carbon-containing precursors including combustion and detonation methods,[35–45] mechanical milling,[46,47] carbon ion implantation,[48,49] underwater arc discharge between graphite electrodes,[50–52] annealing of acetylene black in the presence of an iron catalyst,[53] or heating of a carbon filament in liquid alcohol.[54] Alternatively, carbon onions can also be derived *via* phase transformation of nanodiamonds by annealing in vacuum,[55–61] argon,[32,62–67] nitrogen,[68] hydrogen,[69] or helium,[27,70–75] plasma spraying of nanodiamonds,[76] laser irradiation of nanodiamonds in liquid alcohol,[77] electron beam irradiation of carbon materials,[30,78,79] or direct plasma treatment of coal.[80] The type of precursor and the synthesis conditions have a strong impact on the structure, as seen from transmission electron micrographs of different types of carbon onions given in Fig. 2, but all carbon onions share the multi-shell fullerene-like architecture.

In 1992, Daniel Ugarte observed the formation of carbon onions during electron beam irradiation of amorphous carbon particles in a transmission electron microscope (TEM).[30] Due to irradiation-stimulated graphitization, amorphous carbon can be transformed to nanometer-sized carbon onions with clearly visible nucleation centers (Fig. 2I). While scientifically intriguing, this method is limited in terms of the yield of synthesized carbon onions.[30]

The production of carbon onions *via* decomposition of carbon-containing precursors like CH_4 in the presence of Ni/Al composite catalysts (Fig. 2D) can be accomplished at rather moderate temperatures of 600 °C in hydrogen.[37] The resulting carbon onions showed a hollow structure with several carbon shells and a diameter larger than 30 nm. The catalytic decomposition enabled the formation of carbon onions with a metallic core. Hou *et al.* used a counterflow diffusion flame method (Fig. 2A) to obtain carbon onions on a nickel catalyst.[39] By mixing ethylene, methane, nitrogen, and oxygen, it was possible to control the yield as well as the size of carbon onions.[39] These synthesis methods, together with boron-doped carbon onions from chemical vapor deposition (Fig. 2P),[36] the carbonization of phenolic resin with ferric nitrate (Fig. 2F),[42] and carbon ion implantation in copper and silver (Fig. 2N),[48] present facile ways for the production of carbon onions, but may be disadvantageous due to a high amount of hetero-atoms in the product.

In a study by Choucair *et al.* (Fig. 2B), high purity carbon onions with more than 90 mass% carbon and no metal impurities were produced by a catalyst-free flash pyrolysis of naphthalene.[40] The particles of *ca.* 50 nm diameter were composed of highly defective carbon shells, as shown by Raman spectroscopy and TEM. Gao *et al.* (Fig. 2C) used laser-assisted combustion of C_2H_4 in air.[81] The resulting high purity carbon onions with a diameter of *ca.* 5 nm exhibited a high degree of sintering and the KOH activated materials showed a promising supercapacitor performance with a capacitance of up to 126 F g^{-1} in 2 M KNO_3 and a relatively high surface area of up to 804 m^2 g^{-1} (see Section 4.1 for further discussion).[81]

Underwater arc-discharge-derived carbon onions (Fig. 2M)[52] and nanodiamond-derived carbon onions (Fig. 2E) have been evaluated as electrodes for supercapacitors.[4,82–85] The advantages of these two synthesis methods are the high yield, the high purity, and the good controllability and reproducibility. Yet, not all synthesis routes reported in the context of carbon onion synthesis actually yielded carbon onions as defined above. For example, Fan *et al.* synthesized carbon particles by heating carbon in liquid alcohol; these particles had a nanoscopic size of ~50 nm, but without a multi-shell structure.[54] Structurally, such carbon nanoparticles are virtually indistinguishable from carbon black. Bystrzejewski *et al.* used the thermolysis of a NaN_3–C_6Cl_6 mixture to produce different types of carbon onions (Fig. 2G).[43] In some of their experiments, the multi-shell structure was clearly produced, but large amounts of carbon by-products were generated, too.[43] The same was observed by using ball milling of graphite published by Chen *et al.* (Fig. 2O).[47]

2.2 Nanodiamond-derived carbon onions

Thermal annealing of detonation nanodiamond powders has emerged as the most practical method for producing carbon onions.[8,61] Key benefits are the high purity, the small particle size between 5 nm and 10 nm, large-scale material production with high material homogeneity and a relatively low price of the precursor (currently ~2 € per gram). Further cost reductions are expected as worldwide synthesis capacities for carbon onions are increasing. Furthermore, the facile synthesis of nanodiamond-derived carbon onions is attractive because the material can be obtained by simple thermal treatment in an inert atmosphere (*i.e.*, dry powder processing).[87]

By now, various nanodiamond precursors, heating rates, annealing temperatures, and durations have been investigated. Considering the use of different synthesis atmospheres like vacuum,[55–61] argon,[32,62–67] nitrogen,[68] hydrogen,[69] or helium,[27,70,73–75] it is difficult to adequately compare the structure and properties of the resulting carbon onions. Typically, detonation nanodiamonds with a mean particle size of *ca.* 5 nm are used as precursors for carbon onion synthesis. Chemically, nanodiamonds consist of 80–90 mass% of carbon, a few mass% of oxygen, hydrogen, nitrogen, and minor amounts of other impurities.[32,88,89] Oxygen and hydrogen are associated with surface functional groups, whereas nitrogen can also be located in the nanodiamond core.[88] The detonation synthesis of nanodiamonds yields particles engulfed by a thin layer of amorphous and disordered carbon.[88,90–92] It also leads to particle agglomeration and sintering with agglomerates of several hundreds of nanometers.[93]

The thermal transformation of nanodiamonds to carbon onions is a multistep process. In general it starts with desorption of water and detachment of oxygen-containing surface functional groups from sp^3-hybridized carbon when heating up to around 200 °C.[94–96] Further increasing the temperature will

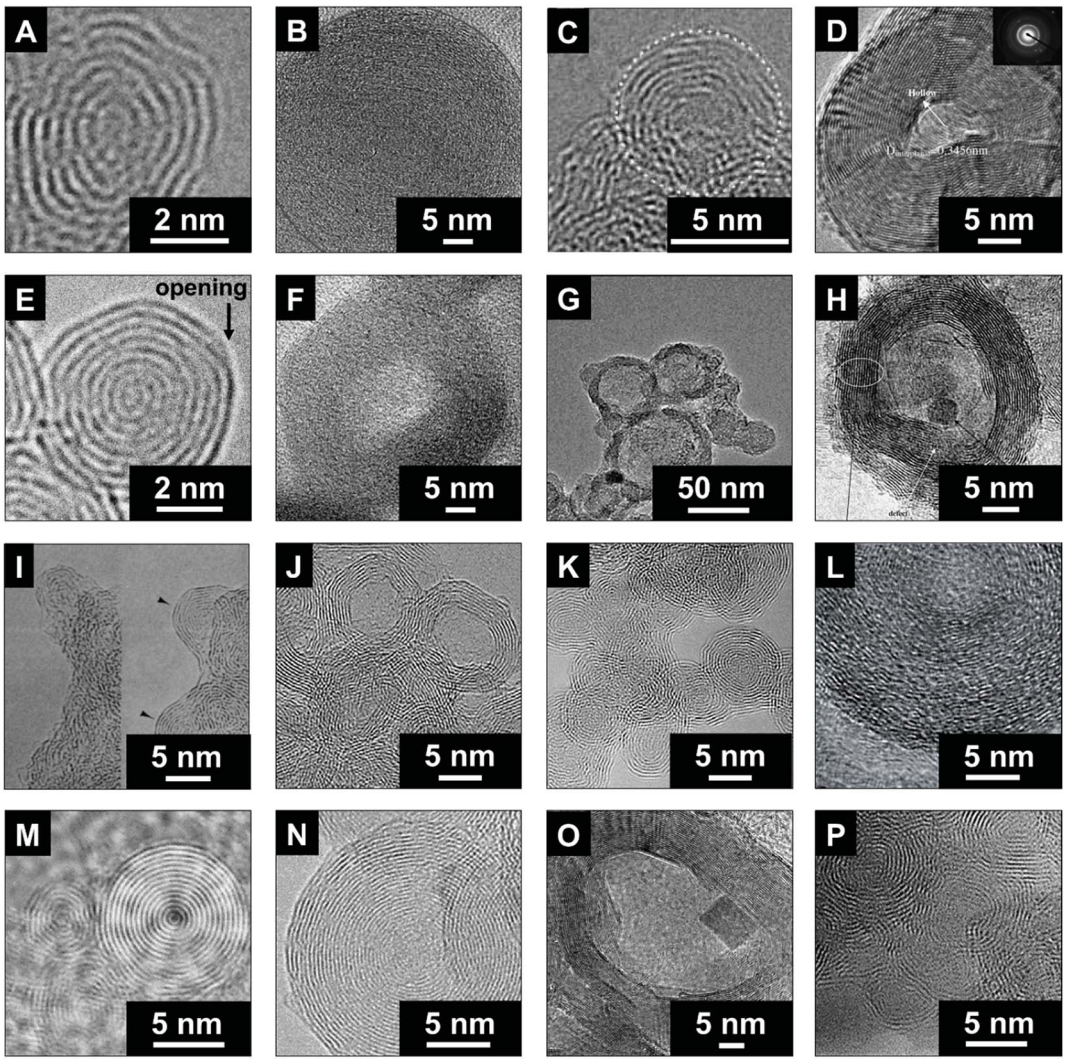

Fig. 2 Transmission electron micrographs of carbon onions synthesized using different methods. (A) Hou *et al.*, counterflow diffusion flame method (with permission from Elsevier);[39] (B) Choucair and Stride, flash pyrolysis of naphthalene (with permission from Elsevier);[40] (C) Gao *et al.*, laser-assisted combustion process using C_2H_4 and O_2 (with permission from IOP Publishing);[41,81] (D) He *et al.*, catalytic decomposition of C_2H_4 on Ni/Al (with permission from Elsevier);[37] (E) this work, annealing of nanodiamonds; (F) Zhao *et al.*, carbonization of phenolic resin in the presence of ferric nitrate (with permission from Elsevier);[42] (G) Bystrzejewski *et al.*, thermolysis of a NaN_3–C_6Cl_6 system under argon or air atmosphere (with permission from Elsevier);[43] (H) Lian *et al.*, annealing of acetylene black in the presence of ferric nitrate (with permission from Elsevier);[53] (I) Ugarte, electron-beam irradiation of amorphous carbon (with permission from Macmillan Publishers);[30] (J) Du *et al.*, radio frequency plasma treatment of coal (with permission from Elsevier);[80] (K) Xiao *et al.*, laser irradiation of nanodiamonds in liquid alcohol (with permission from American Chemical Society);[77] (L) Azhagan *et al.*, burning ghee (with permission from The Royal Society of Chemistry);[86] (M) Sano *et al.*, arc discharge between graphite rods in water (with permission from Macmillan Publishers);[52] (N) Cabioc'h *et al.*, carbon ion implantation in copper and silver (with permission from Elsevier);[48] (O) Chen *et al.*, ball milling of graphite (with permission from Elsevier);[47] (P) Serin *et al.*, chemical vapor deposition using BCl_3, C_2H_2, and H_2 (with permission from Elsevier).[36]

effectively remove functional groups like carboxyl, anhydride, and lactone groups, leading to the emergence of CO and CO_2 gases.[32,94,96] Detachment of functional groups causes the formation of dangling bonds on carbon atoms which can reconstruct and combine to form π-bonds, indicating the onset of graphitization when approaching 800–900 °C. The reconstructive phase transformation forms sp^2-hybridized carbon shells on the outside of the nanodiamonds, followed by continuous graphitization to the inside of the particle when increasing the temperature.[32,59,95,97–100] Structural defects of the nanodiamond surface, stemming from the synthesis or from the detachment of surface functional groups, increase the reactivity of surface carbon atoms which greatly facilitates the phase transformation process.[100] At temperatures between 1100 °C and 1300 °C, the initially highly disordered carbon shells become increasingly more graphitic with a lower defect density yielding a fully transformed highly ordered carbon onion at 1800–2000 °C.[55,101] During the phase transformation, if the nanodiamond particles are in direct contact, the dangling bonds of two adjacent particles may combine, forming a common π-bond; thus local particle sintering may occur, facilitated by carbon etching and redistribution at higher

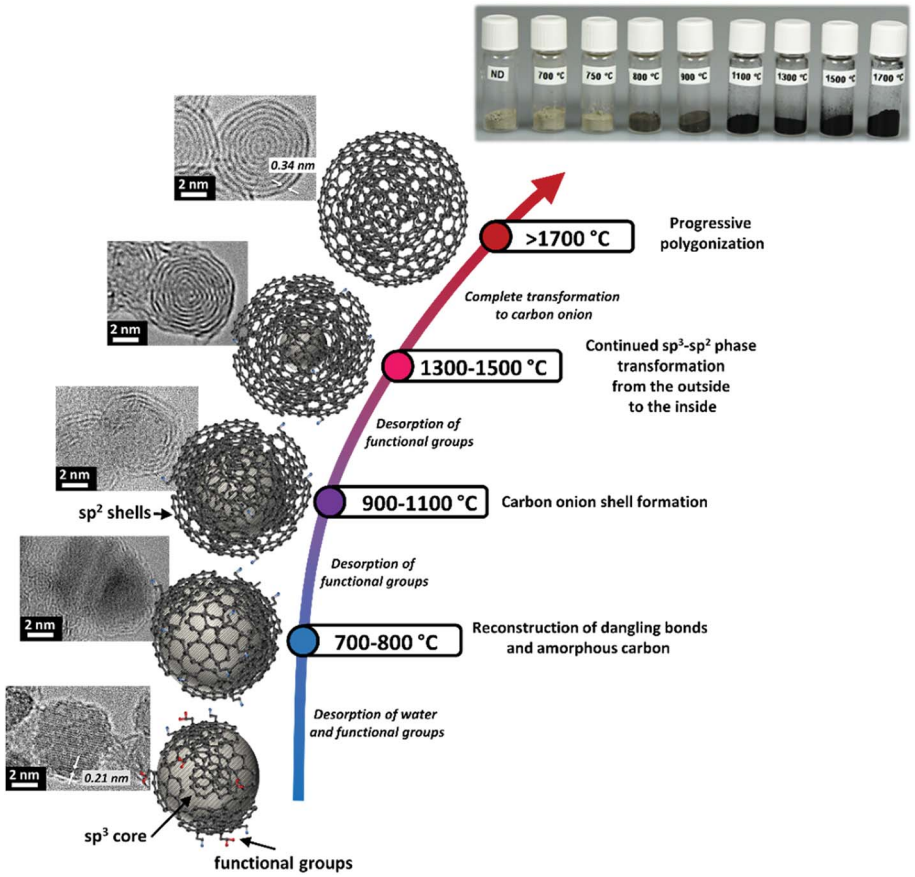

Fig. 3 Transformation from nanodiamonds to carbon onions by annealing shown using transmission electron micrographs, optical images, schematic illustrations of intermediate steps, and the assignment of physical effects depending on the annealing temperature (slight variations occur depending on the annealing atmosphere, especially when comparing vacuum with an inert gas atmosphere).

temperatures. Examples for the different stages of the nanodiamond to carbon onion transformation are given in Fig. 3.

3. Physical and chemical properties of nanodiamond-derived carbon onions

3.1 Properties of nanodiamond-derived carbon onions: overview

A summary of selected physical and chemical properties of nanodiamond-derived carbon onions is given in Fig. 4 in dependence on synthesis temperature. The next sections will address in more detail the structural aspects of the nanodiamond to carbon onion transition and specifically aspects of electrical conductivity and porosity. For electrochemical energy storage, carbon onions synthesized at temperatures of at least 1700 °C present the most attractive set of properties. Due to the high temperature, the nanodiamond transforms completely to carbon onion resulting in a low content of surface functionalities (mostly oxygen-containing functionalities), a low density leading to a relatively high surface area, and a high carbon ordering which is responsible for the high conductivity.

Kuznetsov *et al.* investigated the graphitization mechanism and formulated a model for the gradual phase transition.[61] The exfoliation to graphite sheets preferentially occurs on the (111) diamond facets and involves shrinkage along the graphitic network.[61,104] The decrease in density from nanodiamonds (~3.3 g cm^{-3}) to graphitic carbon (1.9–2.2 g cm^{-3}) induces an increase in particle volume.[32,56,61] Therefore, the number of diamond surface atoms was not sufficient to form a closed shell on the outside of the particle. The missing carbon atoms come from the edges or inner diamond layers leading to the complete closure of carbon onion shells. The transition from nanodiamond to carbon onion might be characterized by intermediate steps, for example spiral-like carbon shells or semi-spherical shells, which are yet to be reliably confirmed in experiments.[61,105,106]

In a theoretical study by Ganesh *et al.*, Reax force field was used to model the transformation from nanodiamonds to carbon onions.[97] In agreement with experimental studies, a step-wise transformation takes place, successively from the outside to the inside when increasing the annealing temperature. A full conversion, for example for a 2 nm nanodiamond, was only reached at 1800 °C. For temperatures below 627 °C, no conversion occurred, in agreement with experimental studies on larger nanodiamond particles.[32,84] It is expected that larger nanodiamonds would show a lower degree of transformation for the same temperature. The simulations yielded highly

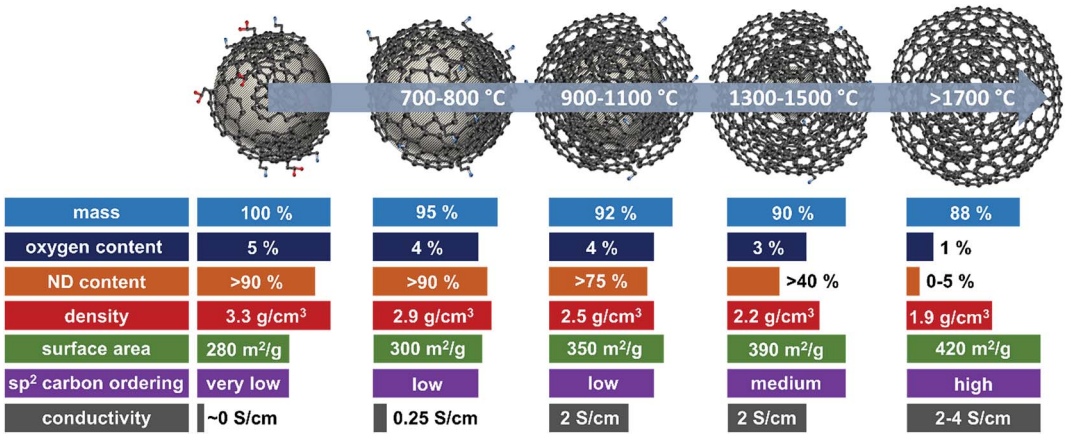

Fig. 4 Properties of nanodiamond-derived carbon onions dependent on the synthesis temperature. The values are approximations shown to demonstrate the trend in selected physical and chemical properties for carbon onions annealed at different temperatures. For more precise values, we recommend the following literature: mass loss and oxygen content,[32,87] ND content,[56,102] skeletal density,[32,56,87] specific surface area (see Fig. 6, Section 3.3), sp^2 carbon ordering,[32,65,83,101,103] and electrode conductivity (see Fig. 7, Section 3.4).

defective shells and an interlayer spacing of 0.34 nm, slightly smaller than 0.35 nm in graphite. This interlayer spacing makes the intercalation of small ions, for example, lithium, into carbon onions possible. Moreover, some of the simulations reported in this work yielded very interesting structures in which the carbon onion resembled a snail shell with one spiral channel going from the surface all the way down to the center of a carbon onion. This structure is in striking contrast to the closed multishell structure thought to be typical for carbon onions before and may change our perception of ionic and other species intercalation into the carbon onions.[97] Large spiraling channels, which would also allow the uptake of larger ions, are sometimes observed in experimental studies (Fig. 2E).[97,107,108]

3.2 Nanodiamond to carbon onion transformation

The physical and chemical properties of nanodiamond-derived carbon onions strongly depend on the precursor, the synthesis conditions, and the post-synthesis treatment. Both annealing of nanodiamonds in vacuum and inert gas lead to the transformation to carbon onions.[55,87,109] X-ray diffraction (XRD) shows for vacuum and inert gas annealing the emergence of the (002)-graphite peak for temperatures higher than 900 °C, whose intensity increases during annealing, while the intensity of the (111) diamond peak decreases (Fig. 5A). The phase transformation progresses at a faster rate at higher temperatures and is nearly completed for temperatures higher than 1700 °C, as is indicated by the small (111)-diamond peak (Fig. 5A).[55,87,109]

During the transformation, not only the carbon onion/diamond ratio increases, but also the degree of sp^2 carbon ordering. A high degree of sp^2 carbon ordering is desirable to enhance the electrical conductivity and can be accomplished by using high synthesis temperatures (above 1500 °C). With higher annealing temperature, carbon onions become more graphitic, leading to an increase of the density states of conductive electrons and furthermore to a higher intrinsic conductivity.[111] For spherical carbon onions, consisting of small poorly connected domains of graphitic sp^2-hybridized carbon, dangling bonds due to structural defects were detected using electron spin resonance (ESR). The π-electrons localized in the small graphitic domains might not provide sufficient conductivity. Gan and Banhart showed that spherical carbon onions are highly stable up to temperatures of more than 1200 °C.[112] For comparison, in polyhedral carbon onions, formed at temperatures higher than 1800–1900 °C,[57,83] dangling bonds were reduced and delocalization of π-electrons increased the intrinsic conductivity.[57]

Raman spectroscopy is a powerful tool to characterize the structure of carbon onions.[101,103,113–115] Carbon onion Raman spectra exhibit a G-mode coming from the vibration of carbon atoms in sp^2-hybridized carbon networks and a disordered D-mode related to the breathing of hexagonal carbon rings with defects (Fig. 5B). The G-mode, usually at 1582 cm^{-1} for planar graphite,[116] is commonly downshifted for carbon onions.[113,114] At lower synthesis temperature, such as 750 °C, the Raman spectrum of the material resembles amorphous carbon covering the surface of the particles, similar to the nanodiamond precursor (Fig. 5B).[117] Due to the limited ability to study nanodiamonds with visible light excitation, UV-Raman is often preferred. The UV-Raman spectrum of nanodiamonds is additionally presented in Fig. 5B. For a synthesis temperature of 800 °C, the graphitic G-mode and the disordered D-mode emerge from the nanodiamond starting material, presenting the onset of the transformation to carbon onions (Fig. 5B). The G-mode shows a relatively broad shape due to the large bond length variation in the material. Together with a broad background coming from amorphous carbon at ~1520 cm^{-1} and the emergence of the D-mode at ~1340 cm^{-1}, it can be concluded that the sp^3-hybridized carbon starts to transform into sp^2-hybridized carbon. Higher annealing temperature results in sharper D- and G-modes and lowers the secondary amorphous carbon signal.[87,101]

In general, Raman spectra of carbon onions can often be reasonably well explained assuming at least two different

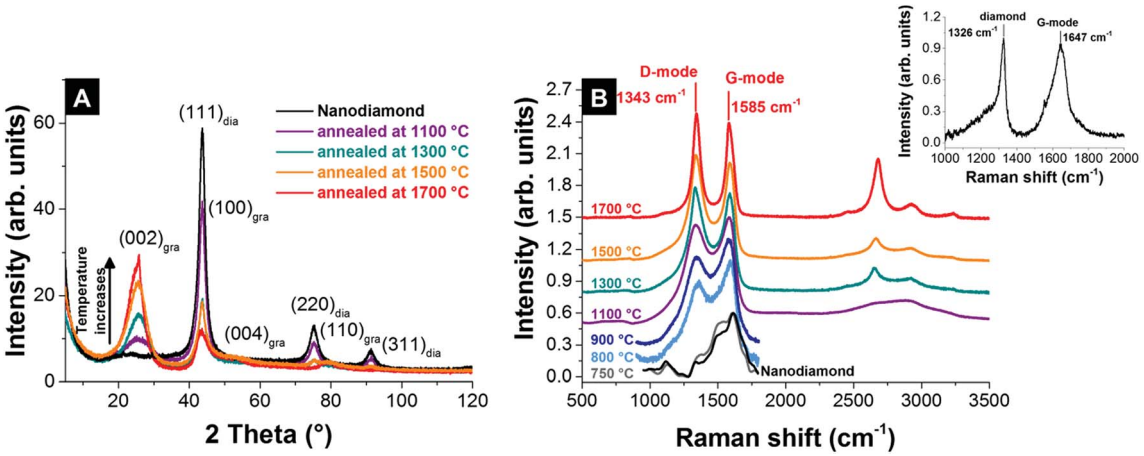

Fig. 5 (A) X-ray diffractograms of nanodiamond and carbon onions synthesized at different temperatures in an argon atmosphere.[32] (B) Raman spectra of nanodiamond-derived carbon onions synthesized in argon measured with a 532 nm laser (recorded using 0.2 mW, 30 accumulations, and 10 s acquisition time; for pristine nanodiamonds and nanodiamonds annealed at 750–900 °C the spectra were only recorded using 1 accumulation to avoid laser-induced heating and were baseline-corrected).[32] The inset shows the Raman spectrum of nanodiamonds measured with a 325 nm UV-laser.[110]

carbon phases present, namely the disordered carbon onion structure rather than a specific spectrum of spherical shells[113] and amorphous carbon.[87] Typically, additional low-intensity Raman modes are observed for wavenumbers below 1000 cm^{-1}. Roy *et al.* discussed these peaks using the 2D phonon density of states (PDOS) and the dispersion curves of graphite.[114]

In addition to XRD and Raman spectroscopy, TEM is a facile tool to image and analyze the nanodiamond to carbon onion transformation (see also Fig. 2).[55,58,61,77,83,101,103,109,118–121] The conversion can be directly performed using electron irradiation of nanodiamond powder in a TEM.[118] The shells form from the outside inward. According to electron energy loss spectroscopy (EELS), sp^2-hybridized carbon forms in this process, but some sp^3-hybridized carbon may remain. Various types of defects in the carbon onion structure were proposed such as holey shells, spiral-like structures, y-junctions, and protuberance, but the experimental investigation of the structure and defects of the shells is difficult.[118]

A key difference between vacuum and inert gas atmosphere annealing is related to the role of surface functional groups. A high oxygen content in nanodiamonds leads to an increased amount of decomposing functional groups, which form gaseous carbon oxides in the reaction zone.[32,122] If the nanodiamond annealing process is carried out in vacuum, the partial pressure of these carbon oxides remains near zero. However, if the process is carried out in an inert gas atmosphere, the partial pressure may stay high enough to cause local carbon etching and effective redistribution of carbon. The extreme case is the formation of micrometer-sized graphitic particles instead of nanometer-sized carbon onions leading to a total loss of the carbon onion structure.[32] Even in less extreme cases, carbon onions from annealing nanodiamonds in an inert gas atmosphere show other characteristic features related to carbon redistribution. As seen from XRD and Raman (Fig. 5A and B), the material after annealing in an inert gas atmosphere consists of two phases: nanometer-sized carbon onions and few-layer graphene nanoribbons (Fig. 6A and B). In contrast, a second carbon phase (*i.e.*, nanoribbons) is absent in carbon onions from vacuum annealing (Fig. 6C and D).[87]

3.3 Porosity characteristics of nanodiamond-derived carbon onions

Unlike many other carbon materials for electrochemical energy storage (*e.g.*, activated carbons), a relatively large surface area of nanodiamond-derived carbon onions is commonly believed to be entirely associated with their external surface. The typical

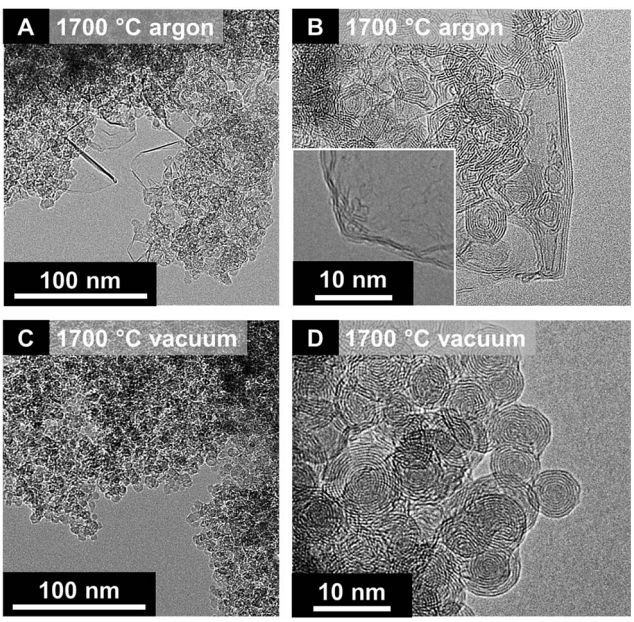

Fig. 6 Transmission electron micrographs of nanodiamond-derived carbon onions synthesized at 1700 °C in argon (A and B) and vacuum (C and D). Reproduced with permission from Elsevier from ref. 87.

values of specific surface area are 300–600 $m^2 g^{-1}$ (Fig. 7A) with more than 1 $cm^3 g^{-1}$ interparticle pore volume.[87] For comparison, activated carbons present usually more than 1500 $m^2 g^{-1}$ specific surface area, with a pore volume also around 1 $cm^3 g^{-1}$.[7] The fully accessible external surface area of carbon onions greatly facilitates ion transport during charge and discharge in electrochemical energy storage devices. This is in contrast to nanopores within micrometer-sized particles (*e.g.*, of activated carbon), as will be shown in Section 4.1. Typically, the pore size distribution (*i.e.*, interparticle pores) of carbon onion powders is relatively broad: from <1 nm up to 40 nm.[32] The surface area of nanodiamond-derived carbon onions strongly depends on the synthesis parameters with maximum values just below 650 $m^2 g^{-1}$ (Fig. 7A). For carbon onions synthesized by certain methods, such as arc discharge of graphite, even higher values can be reached (up to 984 $m^2 g^{-1}$).

To understand the dependency of the surface area on the synthesis conditions, we have to consider that the nanodiamond to carbon onion phase transformation not only brings along a structural change, but also significantly decreases the density.[32,56,97] The density of nanodiamonds (3.3 g cm^{-3}) is much higher than that of carbon onions (*e.g.*, ~1.9 g cm^{-3} for carbon onions produced at 1700 °C).[32] As a result of the large decrease in density, a volume expansion occurs during the formation of sp^2-hybridized carbon shells from the outside to the inside of the particles.[32,56] This expansion has been predicted by modeling and verified experimentally by the increase in surface area (nitrogen gas sorption analysis) and the continuous decrease in density (helium gas pycnometry).[32] The higher lattice spacing of graphite compared to diamond leads to a decrease in density, a volume expansion, and to an increase in specific surface area (Fig. 7B). By normalizing the surface areas of different nanodiamond-derived carbon onions to the surface area of the precursor nanodiamonds, one can determine a constant increase in surface area up to around 70% when annealing at 1500 °C. For temperatures higher than 1500 °C, the surface area does not increase and may even decrease, whereas the density keeps decreasing.[32] Locally occurring particle–particle sintering, as well as carbon etching and redistribution to larger structures, is an important factor for the decrease in surface area. At the end of this process, even consolidated structures in the form of micrometer-sized graphitic particles may occur when using an inert gas atmosphere for the synthesis.[32,122]

To increase the surface area of carbon onions beyond the values of ~600 $m^2 g^{-1}$, chemical or physical activation can be used, such as oxidation in air or acid treatment. So far, the highest value for activated nanodiamond-derived carbon onions was ~650 $m^2 g^{-1}$ using oxidation in air (corresponding to an increase of the surface area by 100% compared to the surface area of the nanodiamond precursor).[32] The increase in the surface area is accomplished by the removal of interparticle pore-blocking amorphous carbon and a partial decrease in the carbon onion diameter.[32] Higher values of the specific surface area above 800 $m^2 g^{-1}$ were achieved by KOH activation of carbon onions produced by laser-assisted combustion of methane.[81] Compared to oxidation in air, KOH etching does not remove carbon shells and amorphous carbon; rather this procedure etches new pores into the carbon onions.[81] The largest surface area reported so far is 984 $m^2 g^{-1}$ by using an arc-discharge method with graphite as the precursor and this high value was explained by the emergence of intraparticle pores due to surface roughening.[123] In the latter study, TEM images showed particles with a diameter of 4–36 nm which is up to 4-times larger than for nanodiamond-derived carbon onions. The rather low density of 1.64 g cm^{-3} may also indicate the presence of other carbon nanoforms in the sample (which is common for this type of synthesis method). Thus, it is difficult to tell to what extent this large specific surface area of the products can be assigned just to carbon onions.

Until now, the discussion was limited to surface area and pore volume, but ion accessibility to a certain pore can only be

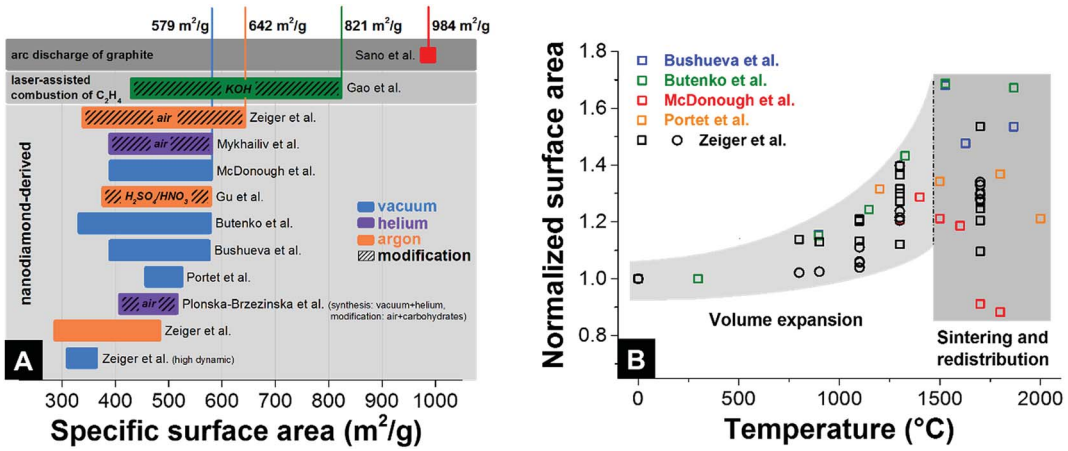

Fig. 7 (A) Surface areas of different types of carbon onions. The colored bars give the range in surface area with minimal and maximum values. See the legend for synthesis atmosphere and post-synthesis modification. Bushueva *et al.*,[84] Butenko *et al.*,[56] McDonough *et al.*,[83] Portet *et al.*,[4] Zeiger *et al.* (circle and square symbolize 2 different nanodiamond precursors),[32,87] Sano *et al.*,[123] Gao *et al.*,[81] Mykhailiv *et al.*,[70] Gu *et al.*,[124] Plonska-Brzezinska *et al.*[75] (B) Relative change of surface area during annealing of nanodiamond in an inert gas or vacuum.

understood when we consider the actual pore size distribution (PSD). The PSD can be derived from gas sorption isotherms using, for example, CO_2 at 0 °C (for pores between *ca.* 0.3 and 1.0 nm) and N_2 at −196 °C (for pores between *ca.* 0.6 nm and 30 nm). A slit-shaped pore model is typically assumed as the best-fit model for carbon onions among the available density functional theory (DFT) models.[65] Assuming a series of pores, the PSD of carbon onions can be defined as pores between particles in direct contact (<1 nm), pores between several particles (1–10 nm), and pores between agglomerates (larger than 2 nm).[32] The large number of mesopores with the size 2–50 nm facilitate ion transport which makes carbon onions a very attractive high-power material for supercapacitor electrodes.

3.4 Electrical conductivity of nanodiamond-derived carbon onion electrodes

The electrical conductivity of carbon onion electrodes is influenced by the intrinsic electrical conductivity of the material, the degree of particle sintering, the particle arrangement and compaction, as well as the electrode preparation (*e.g.*, use of binder *vs.* binder-free electrodes). The intrinsic conductivity of carbon onions can be tuned by adjusting the annealing temperatures. High temperatures (>1700 °C) result in a higher degree of carbon ordering. The resulting carbon onions are more graphitic and more electrically conductive (see also Section 3.2 and Fig. 4).[111] The particle sintering is typically caused by agglomeration of nanodiamonds, and partially provoked by high annealing temperatures.[32,125] In a recent study it was shown that annealing in argon instead of vacuum produces few-layer graphene flakes between the carbon onions, which enhance the electrode conductivity.[87]

The electrical conductivity of nanodiamond-derived carbon onion electrodes may reach *ca.* 4 S cm^{-1} measured with a four-point probe on pellets or polymer-bound electrodes.[4] However, the spread of reported values is very large, ranging from below 0.5 S cm^{-1} to above 4 S cm^{-1} (Fig. 8A). The maximum conductivity of ~4 S cm^{-1} (2.5–3 S cm^{-1} for polymer-bound electrodes) is comparable to that of carbon black (*ca.* 1–2 S cm^{-1}) and an order of magnitude higher than activated carbon (<0.5 S cm^{-1}).[4] A comprehensive and fair comparison of experimental data is complicated by the use of different synthesis temperatures, atmospheres, and different electrode preparation methods in the literature. For example, polytetrafluoroethylene (PTFE)-bound film electrodes and compressed pellets show significant differences in conductivity. However, we can assume an increased electrical conductivity for carbon onions synthesized

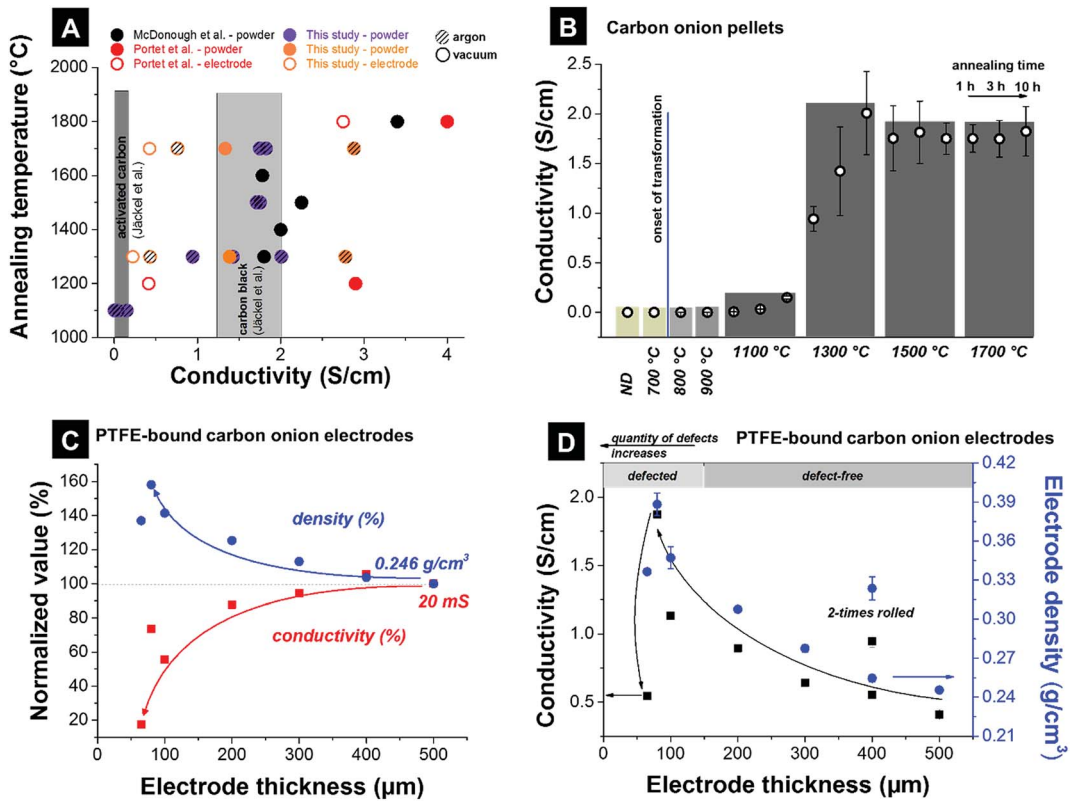

Fig. 8 Conductivities measured using a 4-point probe. (A) Literature values. McDonough *et al.*: powder compressed with 8 MPa;[83] Portet *et al.*: Teflon cylinder filled with powder, copper electrodes of 22 mm in diameter as probes, electrodes with 15 mass% PTFE (mass density 15 mg cm^{-2}) were painted on a current collector covered with conductive paint;[4] this study: ~200 mg powder compressed with 0.25 MPa, electrode with 10 mass% PTFE and a thickness of 200 µm; Jäckel *et al.*: electrodes with 5 mass% PTFE for activated carbon and 10 mass% PTFE for carbon black and a thickness of 200 µm (ref. 7). (B) Carbon onion pellet conductivities: powder of ~200 mg compressed with 0.25 MPa. (C and D) Electrode densities, and electrode conductivities of carbon onions synthesized at 1700 °C in argon for different electrode thicknesses (10 mass% PTFE, 60–500 µm thickness).

at higher temperatures as a result of enhanced carbon ordering, as confirmed by the literature. The large spread of literature values shown in Fig. 8A reflects the large influence of the measurement procedure.

To make a comparison within a cohesive data set, we show in Fig. 8B data for the electrical conductivity of compressed pellets. Nanodiamonds were annealed at different temperatures yielding carbon onions above *ca.* 1000 °C. Using a four-point probe, we measured an increase from the negligible electrical conductivity of nanodiamonds around the onset of carbon onion formation (*i.e.*, at around 800–1000 °C). By varying the annealing time (exemplified for 1100 °C and 1300 °C), we see a continuous increase of the electrical conductivity. This corresponds to a continuous transformation of nanodiamond powder to carbon onions. A residual diamond core and less perfect graphitic shells result in lower electrical conductivity. Finally, constant values are seen for synthesis temperatures exceeding 1500 °C where it is assumed that nearly full transformation to carbon onions has occurred within less than 1 h of annealing.

We show in Fig. 8C and D the influence of the electrode thickness with 10 mass% PTFE as the binder and packing density on the electrical conductivity measured by a four-point probe. For electrode thicknesses between 200 and 500 μm, the sheet conductivity (not normalized to the electrode thickness) varies only within ±10%, mirroring a moderate increase in electrode density by *ca.* 25%. Thus, for the electrode thickness values in the range 200–500 μm the sheet conductivity is not significantly influenced by electrode density and thickness. However, for thinner electrodes, the sheet conductivity drops, for example by more than 80% for 60 μm thickness (compared to 500 μm). Fig. 8D presents the conductivity values normalized to the thickness as common in the literature. By decreasing the electrode thickness the normalized conductivity continuously increases. Thin electrodes are commonly obtained by repeated rolling, which leads to a higher degree of particle compaction (*i.e.*, larger contact area) and a possible increase in electrical conductivity. In Fig. 8D, this is exemplified for a 400 μm thick electrode which was rolled two times. In the second rolling step, additional electrode material is used and rolled to a more compact electrode. A higher density is achieved and a higher conductivity can be reached. The nanoscopic size of carbon onions makes it quite difficult to prepare PTFE-bound electrodes with a thickness smaller than 200 μm. Consequently, very thin PTFE-bound electrodes suffer from cracking and similar issues may arise when using other polymer binders and non-freestanding, sprayed electrodes instead of (hot-)rolling. Therefore, in addition to normalizing the electrical conductivity to the electrode thickness (as commonly done in the literature), careful assessment of the electrode density is required when comparing experimental data.

4. Electrochemical properties of carbon onion electrodes

4.1 Carbon onions for electrical-double layer capacitors

The electrochemical performance of carbon onions reflects their physical and chemical properties, as well as the accessible surface area. Nanodiamond-derived carbon onions commonly show capacitance values of up to 52 F g^{-1} in aqueous 1 M H_2SO_4 (ref. 84) and *ca.* 40 F g^{-1} in 1.5 M TEA-BF_4 in acetonitrile (ACN) (Fig. 9).[4] Chemical and physical activation can be used to improve the relatively small capacitance (for comparison, activated carbon has >100 F g^{-1}) by increasing the surface area. Using a laser resonant excitation of ethylene molecules, carbon onions with a size between 5 nm and 50 nm were produced. For KOH activated carbon onions mentioned before, with surface areas in excess of 800 m^2 g^{-1} an enhanced capacitance of 115 F g^{-1} was achieved in 2 M KNO_3.[81] Carbon onions from the arc-discharge of graphite electrodes have shown a very low capacitance of *ca.* 5 F g^{-1} probably due to the low surface area of particles with a diameter of 25–35 nm.[82] The overall moderate surface area of carbon onions results in a rather low energy storage capacity compared to nanoporous carbons, such as activated carbon or carbide-derived carbon with typical values of 100–200 F g^{-1} (and surface areas above 1500 m^2 g^{-1}).[14] However, the facile ion access to the external surface of carbon

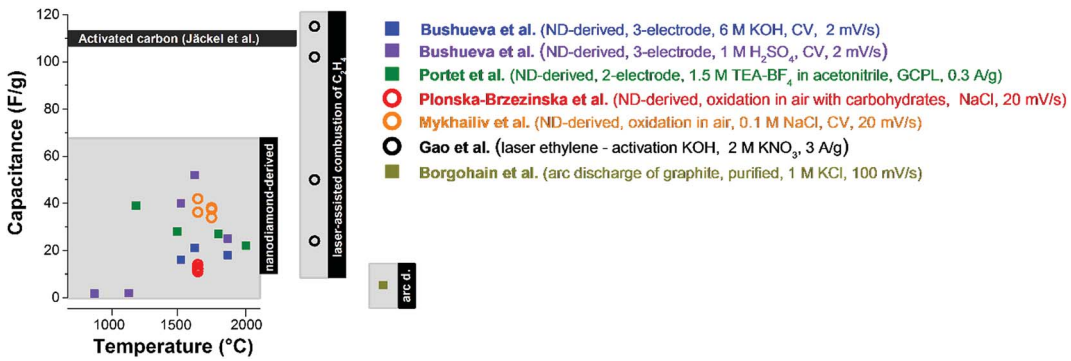

Fig. 9 Capacitance values of different types of carbon onions. Bushueva *et al.*,[84] Portet *et al.*,[4] Plonska-Brzezinska *et al.*,[75] Mykhailiv *et al.*,[70] Gao *et al.*,[81] Borgohain *et al.*[82] The synthesis methods and the settings for electrochemical characterization are presented in the figure. The panel on the left encloses capacitance values of nanodiamond-derived carbon onions, the one in the middle of carbon onions from the combustion of C_2H_4, and on the right of arc discharge carbon onions. Carbon onions without modification are shown by squares and with modification by circles. For comparison, the capacitance of PTFE-bound activated carbon is shown using 1 M TEA-BF_4 in ACN.[7]

onions makes them excel in power handling, as will be discussed in more detail later.

The combination of high intrinsic electrical conductivity (see Section 3.4) and facile ion accessibility *via* an external surface area (see Section 3.3) makes carbon onions very attractive for high power applications that require fast charge and discharge rates (*e.g.*, pulsed operation in hybrid electric cars or power stabilization for grid scale applications).[6] The high intrinsic electrical conductivity of nanodiamond-derived carbon onions is achieved by using high annealing temperatures as discussed in Section 3.4.[4,83,87] The higher degree of carbon ordering not only increases the conductivity and power handling but also leads to higher differential capacitances (*i.e.*, potential-dependent capacitance). In a recent study the influence of carbon ordering on the capacitance of carbon supercapacitors was systematically studied using carbon onions as the model material.[65] Carbon onions with similar porosities, but differing in carbon ordering, were synthesized at 1300 °C, 1500 °C, and 1750 °C in vacuum. Using PTFE-bound electrodes and different organic electrolytes and ionic liquids, the influence of carbon ordering on the electrochemical properties was investigated. Cyclic voltammograms showed a characteristic butterfly shape for all carbon onions, but it was much more pronounced for carbon onions synthesized at high temperatures with a higher degree of carbon ordering (Fig. 10A). The butterfly shape represents an increasing differential capacitance for higher potentials, because the electron density of states changes as a function of applied potential.[65,126] This so-called electrochemical doping[127] strongly depends on the degree of carbon ordering[128] and is enhanced for more ordered carbon onions with higher electrical conductivity. The change in electrical resistance measured with an *in situ* resistance cell is shown in Fig. 10B. At high electrode potentials, the normalized resistance of the electrodes reduces constantly by increasing the annealing temperature.[65]

The nanoscale size of carbon onions necessitates adding more binder during electrode manufacturing, typically 10 mass% PTFE for PTFE-bound electrodes.[7] For activated carbons, usually 5 mass% PTFE is sufficient to prepare free-standing, mechanically stable electrodes.[14] Polymer binders add electrochemically dead mass and may partially block pores leading to lower capacitance.[7] Microcavity electrodes present a facile tool to qualitatively compare different electrode materials without the influence of binders.[4] In a study by McDonough *et al.*, carbon onions synthesized at different temperatures were electrochemically tested using microcavity electrodes in 1 M H_2SO_4.[83] At scan rates up to 15 V s^{-1}, the relative capacitance for carbon onions synthesized at 1800 °C decreased by less than 30% compared to the low-rate value, while carbon onions synthesized at 1300 °C showed a reduction by 45% at 15 V s^{-1} (Fig. 10C). Compared to carbon onions, other carbon materials like activated carbon suffer from a lower degree of carbon ordering and lower ion mobility resulting in a decrease in capacitance of more than 70% under comparable testing conditions. The enhanced power handling ability of carbon onions synthesized at higher temperatures (*e.g.*, 1700 °C *vs.* 1300 °C) was also demonstrated for full cells with 200 μm thick electrodes in galvanostatic measurements.[87] Carbon onions in this study were derived from nanodiamonds *via* vacuum or argon annealing and higher synthesis temperatures led to higher capacitance retention when increasing the specific current.[87] By lowering the electrode thickness to 100 μm an even higher power performance and almost no loss in capacitance at 20 A g^{-1} compared to the low-rate value were reported (Fig. 10D). This again shows the high influence of the electrode design on the resulting electrochemical performance in addition to the intrinsic material properties.

As mentioned in Section 3.2, argon annealing leads to etching and redistribution of carbon onion outer shells and amorphous carbon.[32,87] Oxygen containing gaseous species, formed by the decomposition of functional groups, accumulate in the atmosphere around the sample etching the carbon and redistributing it to form few-layer graphene flakes between the particles (Fig. 6).[65,87,122] This effect was only observed by using ultrafast heating and cooling;[87] lower heating rates resulted in larger graphitic particles.[32] Due to the interconnection of the particles by few-layer graphene, a more open network with higher electrical conductivity was produced with an enhanced capacitance retention of 85% at 20 A g^{-1} (Fig. 10D) for PTFE-bound electrodes (10 mass% PTFE, 200 μm thick).[87]

Taking advantage of the high rate handling capability, carbon onions have been demonstrated as electrode materials for ultrahigh-power micro-supercapacitors.[6] Using an electrophoretic deposition technique, nanodiamond-derived carbon onions produced at 1800 °C were directly deposited onto patterned gold current collectors from an ethanol–water suspension. The electrodes showed ultrafast rate handling behavior in 1 M TEA-BF_4 in propylene carbonate (PC) up to 200 V s^{-1} scan rate.[6] This superior rate handling is partially due to the ultrathin electrode thickness of just a few micrometers; as demonstrated in ref. 6, the rate handling of conventional activated carbon is also severely enhanced for micro-supercapacitors as compared to conventional supercapacitors with much thicker electrodes (150–250 μm). The high rate handling ability of carbon onions was also shown for carbon onion/carbon fiber composite electrodes with a thickness below 50 μm.[129] Using 1 M TEA-BF_4 in ACN, a decrease of 37% of the initial low-rate capacitance was found at 100 A g^{-1} using a full-cell setup (two-electrode geometry) for the composite electrode; for comparison, PTFE-bound electrodes of carbon onions without the highly conductive network of carbon fibers showed a 75% decrease in capacitance already at 50 A g^{-1}.[129]

Electrochemical performance stability is another important parameter for energy storage devices; however, so far, only a few studies provided data in this regard for carbon onions. For example, using micro-supercapacitors with high temperature carbon onions (1800 °C, high vacuum), a capacitance retention of ~100% was maintained after 10 000 cycles at 10 V s^{-1} in an organic electrolyte.[6] Yet, micro-supercapacitor data are not directly transferable to estimate the performance stability of full cells. Two-electrode (full cell) data were provided by another study for the comparison of nanodiamond-derived carbon synthesized at 1300 °C and 1700 °C in argon or high vacuum.[87] While no significant difference in the performance stability was

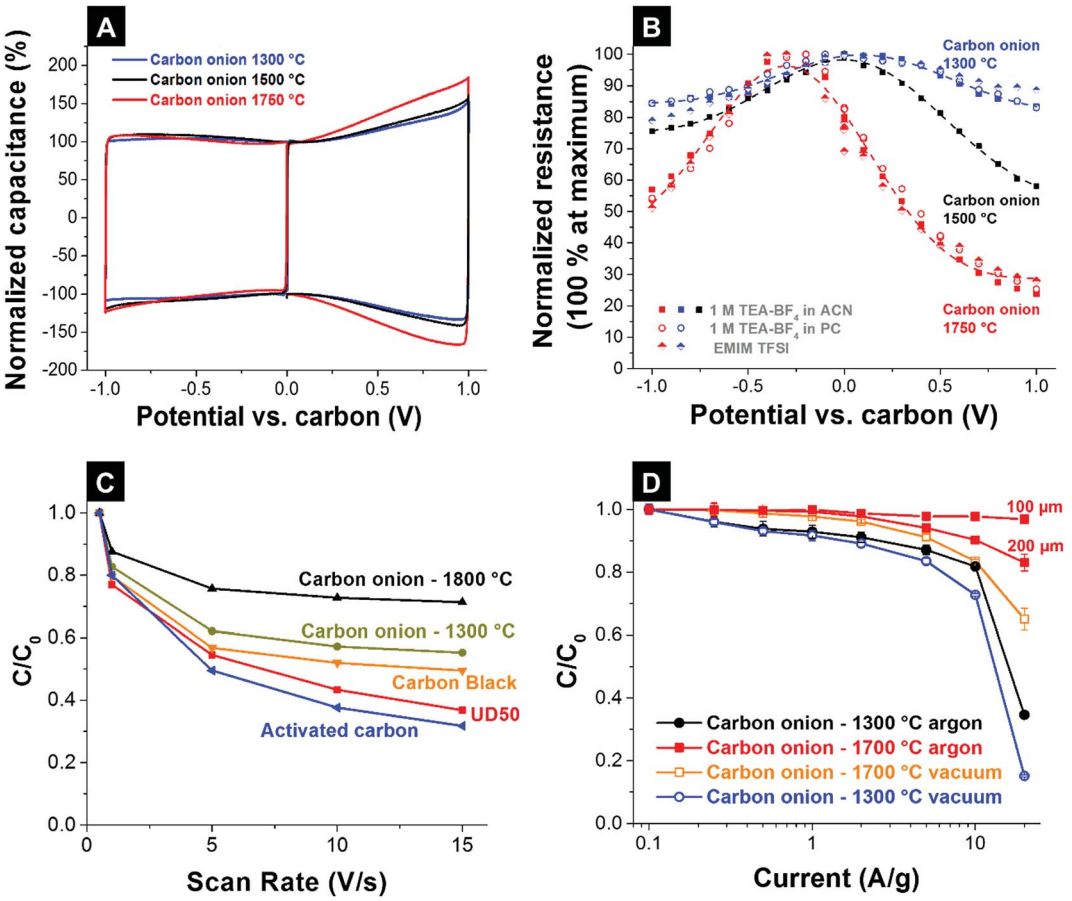

Fig. 10 (A) Cyclic voltammogram of PTFE-bound electrodes, made of nanodiamond-derived carbon onions synthesized at 1300 °C and 1750 °C in 1 M TEA-BF_4 in ACN at 10 mV s^{-1}.[65] (B) Resistance of the carbon onion electrodes after charging to a specific potential using an *in situ* resistivity measurement cell for different electrolytes.[65] (C) Rate handling behavior of the carbon onion powders compared with activated carbon, carbon black, and the nanodiamond precursor (UD50-detonation soot) measured in 1 M H_2SO_4.[83] (D) Rate handling behavior of film electrodes (200 µm, unless stated otherwise) of carbon onions synthesized from nanodiamonds at 1300 °C and 1700 °C in flowing argon or vacuum. All data from ref. 87 were measured in 1 M TEA-BF_4 in ACN using a full cell set-up with a cell voltage of 2.7 V.

caused by using different synthesis atmospheres (vacuum *vs.* argon), a significant difference was identified when comparing the different synthesis temperatures (1300 °C *vs.* 1700 °C). Using voltage floating at 2.7 V in TEA-BF_4 in ACN, high temperature carbon onions still showed nearly 100% capacitance retention after 100 h, while the capacitance of low temperature carbon onions decreased to ~90% after 20 h. These data correlate with the measured charge efficiency, which remains virtually unchanged at around 100% for high temperature carbon onions. The charge efficiency for low temperature carbon onions first decreases to around 92% after 20 h, but then recovers over time to ~98% after 100 h. This effect can be explained by the irreversible reactions of surface functional groups associated with the higher oxygen content after the low temperature synthesis (~3 mass%) compared to the high temperature synthesis (~1 mass%).[87]

In summary, the electrochemical properties of carbon onions depend on the synthesis conditions, as it is typical for carbon materials. Due to the lack of comprehensive electrochemical characterization data for non-nanodiamond-derived carbon onions, the following statements mainly concern carbon onions produced by thermal annealing of nanodiamonds.

- Carbon onions synthesized at higher temperatures (>1500 °C) show a higher degree of carbon ordering, higher differential capacitance for higher potentials, higher conductivity, higher electrochemical stability, and better rate handling capability.

- Typically, low temperature carbon onions (<1500 °C) present higher surface area and higher capacitance due to negligible sintering and carbon redistribution.

- By using rapid heating and cooling rates, sintering can be minimized and high conductivity high surface area carbon onions can be obtained for high annealing temperatures (1700 °C). Improved electrical conductivity, rate handling, and electrochemical stability can be obtained when using an inert gas like argon instead of vacuum for the annealing of carbon onions.

- Activation (*e.g.*, by using KOH) can lead to a roughening of outer shells, development of internal porosity, larger surface area, and accordingly higher capacitance.

- The thickness and packing density of the electrodes strongly influences the rate handling behavior, not only for

carbon onions, but also for other materials and should be taken into account when comparing data.

4.2 Carbon onions as conductive additives for electrical double-layer capacitors

The use of carbon onions as the primary electrode material for electrical double-layer capacitors is limited due to the low energy storage capacity resulting from a low specific surface area (<600 m^2 g^{-1}) when compared to commercial activated carbon.[7] However, their electrical conductivity superior to activated carbon makes them a promising conductive additive, effective in small amounts (typically 5–10 mass%). The very small carbon onions (below 10 nm) as well as their soft agglomerates (typically 100–200 nm) fit into very tight interparticle spaces. This results in a better (more homogeneous) distribution between the micrometer-sized activated carbon particles.[7] As such, carbon onions (1) fill effectively the gaps between larger carbon particles; (2) increase the overall particle–particle contact area between larger nanoporous carbon particles; and (3) decrease the particle–particle resistance since carbon onions are much more conductive than, for example, activated carbon.[7,130,131] Compared to conventional carbon black and graphite nanoparticles, carbon onions consistently lead to a better gravimetric and volumetric performance.[7]

So far, the use of carbon onions as a conductive aid to enhance power handling of carbon supercapacitor electrodes has been documented when admixing to activated carbon,[7,131] mesoporous carbon,[130] electrochemically active polymers,[132] and inserting between graphene oxide sheets.[133] Depending on the added amount of carbon onions, the activated carbon electrode sheet resistance drops by 30–80%.[7] The addition of 10 mass% carbon onions to flexible polyester electrodes leads to a 60% decrease in electrical series resistance.[130] Also, the performance of polymer electrodes based on polyaniline was enhanced by adding carbon onions, yielding an improved cycle stability and better rate handling ability.[132]

4.3 Carbon onions as a substrate for redox-enabled hybrid energy storage

Electrical double-layer capacitors show a high specific power due to fast ion electrosorption on high surface area carbons, but suffer from comparatively low specific energy (commonly around 5 W h kg^{-1} on a device-level).[134] A particularly attractive approach to enhance the energy storage capacity is the implementation of redox-active materials. Carbon onions are highly suited for this task as they are believed to only present an easily accessible external surface, which can be decorated with redox-active species, like surface functional groups, molecular species (*e.g.*, quinones), metal oxides (*e.g.*, manganese oxide), or conductive polymers (*e.g.*, polyaniline, PANI). This is in contrast to highly porous substrates, such as activated carbon, where adding redox-active materials brings along the issue of pore blocking in addition to the poor electrical conductivity of the substrate (especially activated carbon, see Section 3.4). Several types of redox-active species and/or pseudocapacitive materials were used in combination with carbon onions, including manganese oxide,[86,135–137] ruthenium oxide,[26] nickel hydroxide and oxide,[27] PANI,[74,132] poly(3,4-ethylenedioxythiophene):poly(styrenesulfonate) (PEDOT:PSS),[73] polypyrrole,[138] and quinones.[129,139] Among these materials, manganese oxide in combination with carbon onions shows the highest energy storage values with 575 F g^{-1} at 0.5 A g^{-1} in 0.5 M H_2SO_4.[86] A collection of SEM and TEM images of such hybrid materials is given in Fig. 11 and an overview of the capacitance values for redox-enabled carbon onions is presented in Fig. 12.

The vast majority of electrochemical applications of carbon onions relates to their use for supercapacitor electrodes as an active material, conductive additive, or substrate for redox-hybrid systems. In contrast, only a few studies have investigated their use as anode materials for battery systems, such as lithium ion batteries. In a study by Han *et al.*, carbon onions were chemically synthesized at 600 °C by a reaction between copper dichloride hydrate ($CuCl_2 \cdot 2H_2O$) and calcium carbide (CaC_2). The material was tested as an anode material for lithium-ion batteries. In a mixture of 1 M $LiPF_6$ in ethylene carbonate and dimethyl carbonate (EC/DMC, 1 : 1 by volume), carbon onions showed a capacity of 391 mA h g^{-1} at a rate of C/10 after 60 cycles which is slightly larger than the theoretical value of graphite with 372 mA h g^{-1}.[141] This may be explained by a shorter pathway for the ions and the carbon onion structure which exhibits an enhanced number of active sites for Li ion storage.[141] Wang *et al.* hydrothermally coated carbon onions with manganese oxide using $KMnO_4$ at 150 °C for use as lithium-ion battery anodes with a two-electrode configuration, lithium foil as the counter electrode, and 1 M $LiPF_6$ in EC/DMC (1 : 1 by volume) as the electrolyte.[142] The capacity of the manganese oxide composite was increased at 50 mA g^{-1} to ~630 mA h g^{-1} compared to ~260 mA h g^{-1} without carbon onions. The increased rate capability and an improved cycling stability were attributed to the structure of carbon onions leading to fast ion and electron transport.[142] In another publication by Wang *et al.* even 853 mA h g^{-1} was reached with a coulombic efficiency of 98% after pre-lithiation using MoS_2/onion-like carbon composites measured at a specific current of 50 mA g^{-1} in 1 M $LiPF_6$ in EC/DMC (1 : 1 by volume).[143]

4.3.1 Carbon onions decorated with manganese oxide. In a study by Azhagan *et al.*, carbon onions were synthesized by flame burning clarified butter (ghee) and the collected carbon black was annealed at 800 °C in an inert gas to produce graphitic multi-shell carbon onions in the size range of 40–45 nm (Fig. 11A).[86] A microwave assisted hydrothermal reaction with $KMnO_4$ as the precursor was used to coat the carbon onions with manganese oxide. The as-synthesized manganese oxide nanoparticles had a diameter of ~10 nm with the lattice constant of λ-MnO_2 (0.239 nm) measured using TEM. Carbon onion electrodes without metal oxides showed a surface area of 486 m^2 g^{-1} and a capacitance of 171 F g^{-1} at 0.5 A g^{-1} in 0.5 M H_2SO_4,[86] which is 5–10 times higher than that for neat nanodiamond-derived carbon onions from McDonough *et al.*[83] With regard to the presence of a redox peak between −1 V and +1 V, carbon onion surface functional groups may contribute to the enhanced capacitance even in the absence of additional

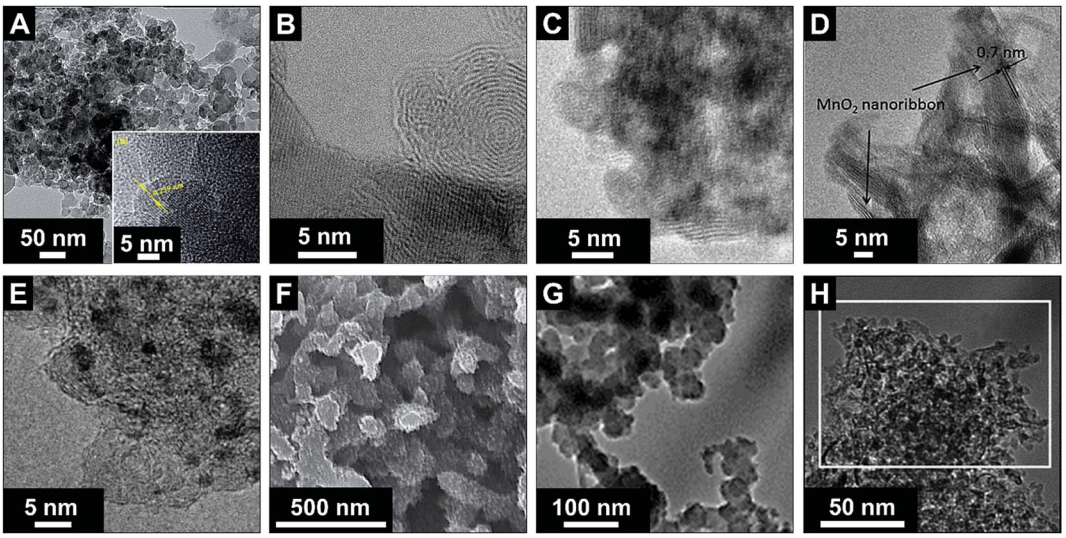

Fig. 11 Transmission and scanning electron micrographs of carbon onions loaded with different types of redox active species. (A–D) Carbon onions decorated with manganese oxide: Azhagan *et al.* (with permission from Royal Society of Chemistry),[86] Makgopa *et al.* (with permission from Royal Society of Chemistry),[135] Borgohain *et al.* (with permission from Royal Society of Chemistry),[136] and Wang *et al.* (with permission from Royal Society of Chemistry);[137] (E) loading with ruthenium oxide: Borgohain *et al.* (with permission from the American Chemical Society);[26] (F) coating with PANI: Kovalenko *et al.* (with permission from John Wiley & Sons Inc.);[132] (G) coating with polypyrrole (PPy): Mykhailiv *et al.* (with permission from John Wiley & Sons Inc.);[138] (H) loading with nickel hydroxide: Plonska-Brzezinska *et al.* (with permission from Royal Society of Chemistry)[27]

decoration with redox-active species (such as quinones or metal oxides). After coating with manganese oxide, the specific capacitance increased to 575 F g^{-1} at 0.5 A g^{-1}, measured in a two-electrode configuration, with a capacitance retention of 18% at 10 A g^{-1}. The relatively low capacitance retention for higher specific current might not only be the result of the low conductivity of the metal oxide coating, but also come from the carbon onion surface functionalities, undergoing irreversible electrochemical transformations at high currents. As shown in ref. 87, high purity carbon onions with a high degree of carbon ordering exhibit superior rate handling with more than 80% capacitance retention even at 20 A g^{-1}. Therefore, the low capacitance retention of the carbon onions before and after their combination with manganese oxide might be the result of large amounts of surface functionalities or the dissolution of manganese oxide in sulfuric acid. Still, the cycle stability after 2000 cycles was more than 90%.[86]

In a study by Borgohain *et al.*, nanodiamond-derived carbon onions were oxidized in sulfuric and nitric acids, and hybrid electrodes of oxidized carbon onions, polydiallyldimethylammonium chloride (PDDA), and delaminated manganese oxide were synthesized by a sequential chemical deposition technique (Fig. 11C).[136] Using a two-electrode configuration and 1 M Na_2SO_4, the highest capacitance of 219 F g^{-1} was reached for the loading with 55 mass% manganese oxide. For comparison, less than 50 F g^{-1} was measured for neat carbon onions.[136] The hybrid electrodes presented a capacitance retention of roughly 80% after 1000 cycles, which is smaller than for the material reported by Azhagan *et al.* with more than 95% after 2000 cycles.[86,136] Borgohain *et al.* used chemical oxidation of carbon onions before they were combined with manganese oxide.[136] Due to the oxidation induced formation of surface functional groups, the stability might be negatively influenced as shown for the as-synthesized carbon onions with a reduction of the capacitance by *ca.* 15% after 1000 cycles. Yet, the decrease was not monotonic: for the first 600 cycles, the capacitance anomalously increased due to faradaic reactions of the surface functional groups and only after their depletion, the capacitance decreased again.[136] A similar effect was found in a study with carbon onions showing reduced stability in an organic electrolyte due to higher contents of oxygen-containing functional groups.[87] The manganese oxide/carbon onion hybrids showed a decrease by *ca.* 15% at 20 mV s^{-1} of the initial low-rate capacitance.[136]

Wang *et al.* used phenolic resin-derived carbon onions hydrothermally coated with manganese oxide in $KMnO_4$ in aqueous solution.[137] In contrast to Borgohain *et al.*, the capacitance did not increase with the manganese oxide loading but rather showed a maximum value of 190 F g^{-1} (galvanostatic mode in 1 M Na_2SO_4) for 80 mass% manganese oxide with a flower-like morphology (Fig. 11D). Up to 2 A g^{-1} in galvanostatic cycling, the electrodes demonstrated good rate handling behavior with more than 93% capacitance retention and almost 100% performance stability over 1000 charge/discharge cycles.[137] For comparison, materials reported by Borgohain *et al.* (219 F g^{-1})[136] and Azhagan *et al.* (575 F g^{-1})[86] had a much lower rate handling ability. These data are in line with a recent study by Makgopa *et al.* using nanodiamond-derived carbon onions and a hydrothermal treatment with $KMnO_4$ producing birnessite-type manganese oxide with a loading of 47 mass% (Fig. 11B).[135] While the as-synthesized carbon onions only showed a capacitance around 30 F g^{-1}, the hybrid electrodes

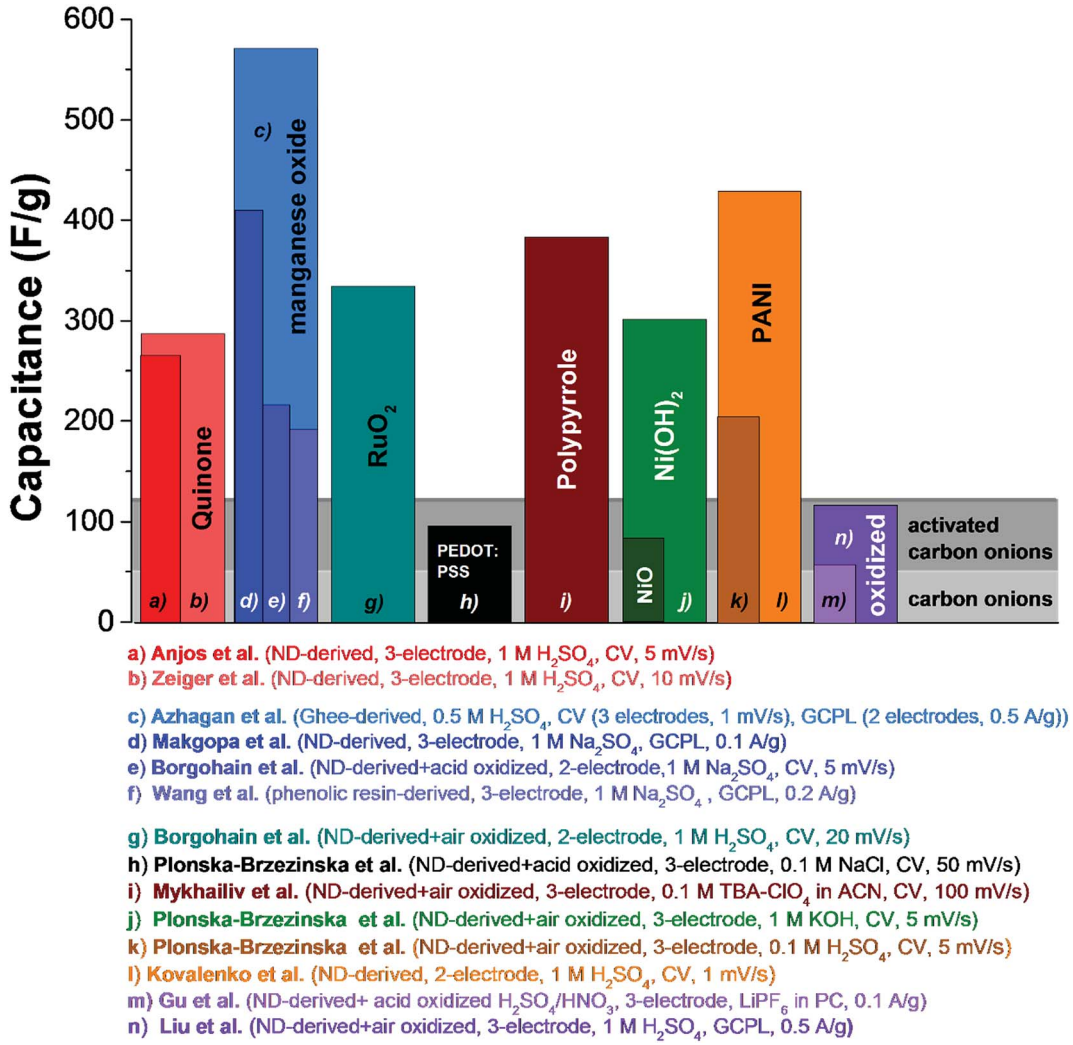

Fig. 12 Comparison of capacitance values of carbon onions decorated with surface functional groups, metal oxides, or conductive polymers. Experimental details are given in the figure. Anjos *et al.*,[139] Zeiger *et al.*,[129] Azhagan *et al.*,[86] Makgopa *et al.*,[135] Borgohain *et al.* (MnO_2),[136] Wang *et al.*,[137] Borgohain *et al.* (RuO_2),[26] Plonska-Brzezinska *et al.* (PEDOT:PSS),[73] Mykhailiv *et al.*,[138] Plonska-Brzezinska *et al.* ($Ni(OH)_2$, the capacitance value in the publication was 1225 F g^{-1}, which is normalized to the carbon content. We adjusted the value by normalization to the electrode mass to compare with other literature values),[27] Plonska-Brzezinska *et al.* (PANI),[74] Kovalenko *et al.*,[132] Gu *et al.*,[28] Liu *et al.*[140]

yielded more than 400 F g^{-1} in 1 M Na_2SO_4 at 0.1 A g^{-1} in a three-electrode setup (Fig. 13A). At higher rates up to 5 A g^{-1}, the material still presents *ca.* 250 F g^{-1} (*i.e.*, 37% decrease).

The rate handling data of several studies of carbon onion/manganese oxide hybrids are shown in Fig. 13B. The plot also shows values for conventional activated carbon and all data are in absolute values so that a direct comparison is possible. Still, a direct quantitative comparison of the rate handling data is difficult due to the different preparation methods and testing setups. For example, Makgopa *et al.*[135] and Wang *et al.*[137] used polyvinylidenefluoride PVDF (5 mass% Makgopa *et al.*, 10 mass% Wang *et al.*) as a binder, with 10 mass% (Wang *et al.*) or 15 mass% (Makgopa *et al.*) carbon black as a conductive additive. The improved charge transport in the presence of a conductive additive (carbon black) complicates a direct comparison of the rate handling data. Moreover, the use of highly graphitic carbon onions with high intrinsic conductivity in the studies by Makgopa *et al.* and Wang *et al.* makes a comparison difficult with other carbon onions, like ghee-derived carbon onions.[86] Also, by the use of carbon onions with a lower electrical conductivity and the absence of an additional conductive additive, the rate handling of the materials reported by Azhagan *et al.* is moderate.[86] While the power handling is limited, the capacitance is very high (575 F g^{-1}), probably due to additional surface functionalities on the carbon onions and the usage of sulfuric acid (oxidizer) as the electrolyte leading to higher values compared to chemically inert electrolytes.[144]

4.3.2 Carbon onions decorated with ruthenium oxide. Ruthenium oxide was also explored as a redox-active coating for carbon onions. Borgohain *et al.* used 5–7 nm nanodiamond-derived carbon onions synthesized at 1650 °C functionalized with polar carboxylic groups.[26] The carbon material was coated with non-agglomerated ruthenium oxide in a hydrothermal reaction using $RuCl_3$ as the precursor (Fig. 11E). Upon loading

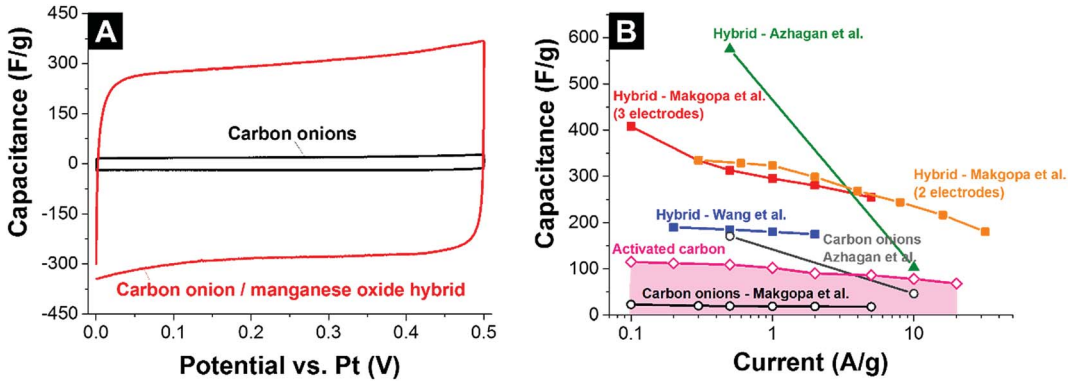

Fig. 13 (A) Cyclic voltammogram of carbon onions and carbon onion/manganese oxide nanohybrids in 1 M Na_2SO_4.[135] (B) Rate handling plot of different types of carbon onions and carbon onion/manganese oxide composites. Makgopa *et al.*: nanodiamond-derived carbon onions coated in a hydrothermal reaction with manganese oxide; 1 M Na_2SO_4 electrolyte.[135] Azhagan *et al.*: burning ghee-derived carbon onions coated using a microwave assisted hydrothermal reaction; 0.5 M H_2SO_4 electrolyte.[86] Borgohain *et al.*: nanodiamond-derived carbon onions were combined with polydiallyldimethylammonium chloride (PDDA), and delaminated-manganese oxide by a sequential chemical deposition technique; 1 M Na_2SO_4 electrolyte.[136] Wang *et al.*: phenolic resin-derived carbon onions were hydrothermally coated with manganese oxide; 1 M Na_2SO_4 electrolyte.[137] Activated carbon electrodes were prepared using 5% PTFE as a binder and measured in 1 M Na_2SO_4 using a full cell set up.

of ruthenium oxide, the surface area decreased from 369 $m^2\ g^{-1}$ for functionalized carbon onions to 126 $m^2\ g^{-1}$ for carbon onions with 68 mass% ruthenium oxide. Accordingly, the capacitance increased up to 334 F g^{-1} for the highest loading of ruthenium oxide measured in 1 M H_2SO_4 by cyclic voltammetry using a full cell setup and a scan rate of 20 mV s^{-1}. The material exhibited excellent power handling when increasing the scan rate from 50 mV s^{-1} to 8 V s^{-1} with nearly ideal capacitance retention.[26] The combination of high electrical conductivity and enhanced surface area (carbon onions) with redox active species (high faradaic charge storage capacity) benefitted improved accessibility of the redox material and allows taking full advantage of the high ion mobility provided by carbon onions. De-agglomerated RuO_2 nanoparticles in the size range of 2–3 nm have a very high surface-to-volume ratio leading to a large ratio of accessible surface to mass per particle. Facile accessibility of the metal oxide nanoparticles to the electrolyte, combined with the good electrical connection to the conductive carbon substrate, enabled a high rate handling behavior. This is paralleled by high performance stability (almost 100% capacity retention after 3000 charge/discharge cycles).[26] In contrast, acid-oxidized carbon onions in the same study without metal oxide decoration underwent irreversible redox reactions due to the surface functional groups and only show ~85% capacitance retention after 3000 cycles.[26]

4.3.3 Carbon onions decorated with nickel oxide. Plonska-Brzezinska *et al.* have explored nickel oxide (hydroxide)/carbon onion hybrids.[27] In one of their studies, nanodiamond-derived carbon onions synthesized at 1650 °C were further oxidized in air to remove amorphous carbon. The resulting carbon onions were loaded with nickel hydroxide nanoparticles (mass ratio *ca.* 4 : 1) in the presence of different modifiers, polyvinylpyrrolidone (PVP), (4-dimethylamino)pyridine (4-DMAP), and pyridinium *p*-toluenesulfonate (PPST). Through further annealing, the composite was transformed to carbon onion and nickel oxide (mass ratio *ca.* 4 : 1). Maximum capacitance values measured in a three-electrode configuration in 1 M KOH at 5 mV s^{-1} scan rate were 306 F g^{-1} for $Ni(OH)_2$ and 73 F g^{-1} for NiO hybrid electrodes with carbon onions. These values were normalized to the total electrode mass to enable a direct comparison with the literature; in the original paper, the reported values of 1225 F g^{-1} and 291 F g^{-1} were normalized only to the carbon content which accounts for ~25 mass% of the total electrode mass. The adjusted values align with values reported for other redox-active hybrid systems, such as a high mass loading of ruthenium oxide (334 F g^{-1})[26] and manganese oxide composites (190 F g^{-1} (ref. 137) to 575 F g^{-1} (ref. 86)). Rate handling was determined by cyclic voltammetry for the hybrid electrodes of carbon onions and $Ni(OH)_2$ or NiO carbon onion composites from 5 mV s^{-1} to 30 mV s^{-1} with a drop in capacitance of ~40% when using $Ni(OH)_2$ and ~6% for NiO. The latter presented promising power handling but suffers from a low 73 F g^{-1} initial capacitance. In contrast, $Ni(OH)_2$ was characterized by a much higher initial capacitance (300% higher) but has relatively poor power handling.

4.3.4 Carbon onions decorated with quinones and functional groups. Redox-active surface species like quinones can significantly enhance the energy storage capacity (preferably in acidic electrolytes).[145] Such systems often do not qualify as pseudocapacitors because their charge-*versus*-voltage is not linear (*i.e.*, non-capacitive), so the use of Farad as a unit has been questioned recently to characterize the capacity of such redox-active energy storage materials.[17,22] However, in order to be able to compare the literature data, we still report in this review values in F g^{-1}.

In a study by Anjos *et al.*, nanodiamond-derived carbon onions were decorated with different types of quinones and tested in 1 M H_2SO_4 in a three-electrode setup.[139] According to the quasielastic neutron scattering experiments by Chathoth *et al.*, quinones arrange parallel to the carbon onion surface due to π interactions between the aromatic rings of the quinones and the carbon planes.[146,147] By scanning from 0.1 V to 0.8 V

versus standard hydrogen, a redox peak was seen between 0.4 and 0.5 V due to a proton coupled electron transfer reaction.[148] The highest capacitance of 264 F g^{-1} was reached in cyclic voltammetry at 5 mV s^{-1} when using 9,10-phenanthrenequinones.[139] The rate handling behavior of these electrodes is rather moderate with only 75 F g^{-1} (*i.e.*, −72%) at 1 V s^{-1} but, in absolute numbers, still better than for activated carbon (*ca.* 20 F g^{-1} at that rate).[129,139] In addition, the performance stability was demonstrated to be high, with the capacitance retention more than 90% after 10 000 charge/discharge cycles.[139] Using nanodiamond-derived carbon onions embedded in a continuous network of conductive carbon nanofibers and 9,10-phenanthrenequinones, the reported capacitance reached values of 288 F g^{-1} at low scan rates and an enhanced power handling could be utilized (135 F g^{-1} at 1 V s^{-1} = −53%).[129]

The cyclic voltammograms of the carbon fiber/carbon onion composite electrodes decorated with different amounts of quinones are shown in Fig. 14A. The redox peak at *ca.* −0.2 V *vs.* Pt increased in area when quinone loading is increased, reaching 288 F g^{-1} capacitance.[129] For a better comparability, Fig. 14B provides an overview of the rate handling ability for different quinone-decorated carbon onion systems (data from cyclic voltammetry). As can be seen, the capacitance retention for carbon onion/carbon fiber composites nears 100% at high scan rates (2 V s^{-1}) and even though the absolute value is rather moderate (34 F g^{-1}) it is still higher than what can be achieved at this scan rate for conventional activated carbon (3 F g^{-1}) using the same set-up and electrolyte system. Loading with quinones increased the capacitance at low scan rates to a maximum value of 288 F g^{-1} at 1 mV s^{-1},[129] which is more than 2 times higher than 115 F g^{-1} for activated carbon at the same rate. For a higher scan rate of 1 V s^{-1}, the capacitance values were still 135 F g^{-1} (ref. 129) and 75 F g^{-1}.[139] Testing over 10 000 cycles demonstrated sufficient stability for quinone-decorated carbon onions and quinone-decorated carbon onion/carbon fiber composites with *ca.* 95% (ref. 139) and *ca.* 90% (ref. 129) capacitance retention, respectively (Fig. 14C).

Apart from loading carbon onions with redox-active or pseudocapacitive materials, an *in situ* electrochemical oxidation of carbon onions in an acidic electrolyte can lead to enhanced capacitive behavior. Liu *et al.* used nanodiamond-derived carbon onions and oxidized them in 1 M H_2SO_4 at a potential from 1.0 to 2.0 V *vs.* Ag/AgCl.[140] The cyclic voltammograms are shown in Fig. 14D. After the first oxidation cycle, the current increases with a maximum at ∼0.3 V and further develops until a capacitance of 99 F g^{-1} (120 F g^{-1} for galvanostatic cycling at 0.5 A g^{-1}) was reached.[140] Due to the insignificant change in specific surface area after electrochemical oxidation, the redox peak is seemingly related to redox-active oxygen functionalities (most probably the quinone–hydroquinone redox couple), which is generated at exfoliated graphene segments of the carbon onions.[140] This assumption is supported by the higher oxygen contents for electrochemically oxidized carbon onions measured with X-ray photoelectron emission spectroscopy (XPS).[140] However, with the higher content of functional groups, the capacitance at higher scan rates decreased to 75 F g^{-1}, which is comparable to what was found for quinone-decorated carbon onions (Fig. 14B).[139] The electrochemical stability was tested for 1000 cycles with nearly 100% capacitance retention in this range. After treating nanodiamond-derived carbon onions in a H_2SO_4/HNO_3 3 : 1 mixture to prepare surface oxidized carbon onions the surface area increased from 384 m^2 g^{-1} to 578 m^2 g^{-1}. Carbon onion shells were etched, interparticle amorphous carbon was removed, and the oxygen content increased from 0.5 at% to 18.3 at%.[124] Electrochemical characterization was performed in a two-electrode coin cell using 1 M lithium hexafluorophosphate ($LiPF_6$) in a 1 : 1 : 1 mixture of dimethyl carbonate (DMC), diethyl carbonate (DEC) and ethylene carbonate (EC), or 1 M $LiPF_6$ in PC.[124] The capacitance values for oxidized carbon onions measured in 1 M $LiPF_6$ in PC are shown in Fig. 14B. The capacitance more than doubled after oxidation compared to untreated carbon onions for all electrolytes. Even when the values were normalized to the enhanced surface area after oxidation, oxidative treatment still increased the normalized capacitance due to redox contributions.[124] However, compared to carbon onions with other surface functionalizations (Fig. 14B) or activated carbon, these values are rather small. The reason might be the lower amount of redox-active sites or the necessity for acidic/protic electrolytes.

4.3.5 Carbon onions decorated with electroactive polymers. Electroactive polymers present another attractive group of materials to impart carbon onion electrodes with additional redox-activity. Polyaniline (PANI) is one of the most popular electrochemically active conductive polymers with a high specific capacitance of maximum 430 F g^{-1} in combination with carbon onions.[132] Conductive polymers, including PANI, commonly suffer from slow charge and discharge compared to carbon materials and poor long-term stability due to volume changes leading to mechanical damage and disrupting conductivity.[132] Therefore, a conductive aid is needed, to enhance the conductivity of the composite. In a study by Kovalenko *et al.*, nanodiamond-derived carbon onions were coated with PANI using a wet chemical approach (Fig. 12F).[132] Pure PANI electrodes demonstrated a capacitance of 470 F g^{-1} in 1 M H_2SO_4 using a symmetric two-electrode configuration (Fig. 15A). The long-term stability after 10 000 cycles was rather low with less than 150 F g^{-1} (*i.e.*, −68%).[132] Electrodes composed of PANI and carbon onions (14 mass% carbon onions) present a more ideal capacitive behavior (Fig. 15B) with slightly smaller capacitance (*ca.* 430 F g^{-1}), but with a much better performance stability (*ca.* −3% capacitance after 10 000 cycles).[132] By increasing the carbon onion amount from 3 to 14 mass%, the capacitance of the composite increased but then decreased when using 28 mass%; thus, there seems to be an optimum load with regard to the electrochemically active surface area.[132] The filling of PANI with nanoparticles lead to a toughening of the polymer and a less distinct volume change during cycling. Interestingly, purified non-conductive nanodiamonds (3 mass%) also significantly enhance the electrode performance. This may sound surprising as purified nanodiamonds have a very low electrical conductivity (≪1 S cm^{-1}) and points to nanodiamond-mediated mechanical toughening and surface roughening of the polymer as the dominant

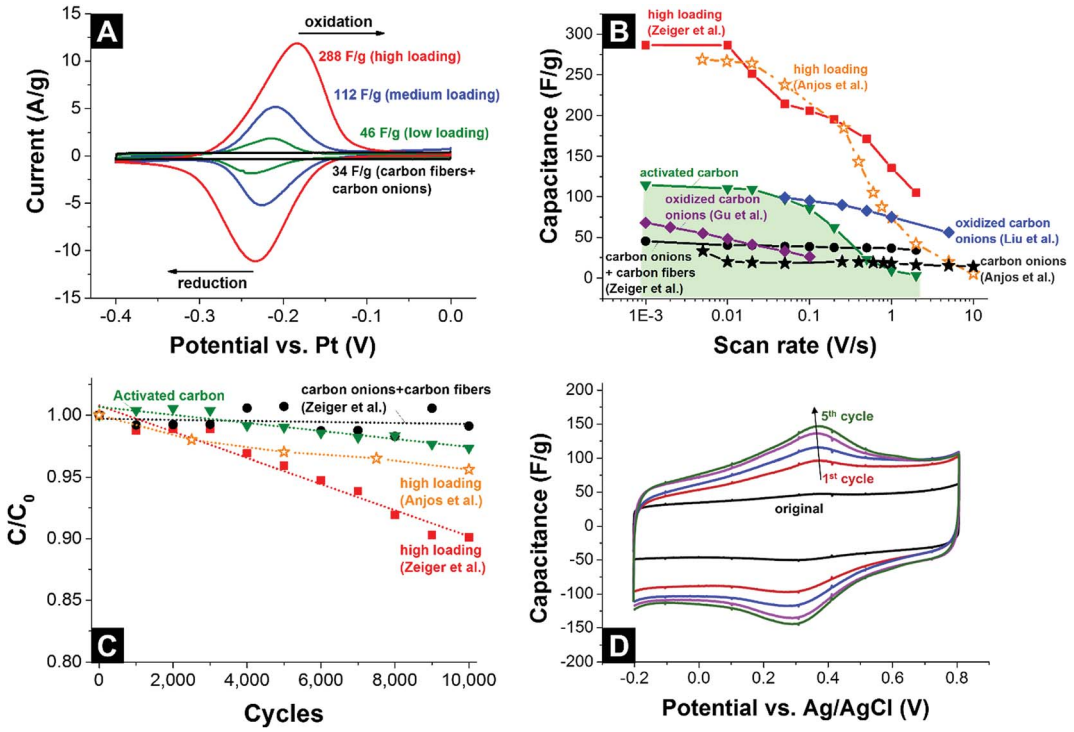

Fig. 14 (A) Cyclic voltammograms of carbon onion/carbon fiber composites loaded with different amounts of 9,10-phenanthrenequinones at 10 mV s^{-1} scan rate.[129] (B) Rate handling data of different types of carbon onions, activated carbon, and carbon onions loaded with quinones or other functional groups. (C) Stability test using 10 000 cycles (CV) with activated carbon, carbon onion/carbon fiber composites, carbon onions and carbon onion/carbon fiber composites loaded with 9,10-phenanthrenequinones. (D) Cyclic voltammograms of carbon onions during electrochemical oxidation. All measurements were performed in 1 M H_2SO_4.[140] Zeiger *et al.*: nanodiamond-derived carbon onion/carbon fiber composites (1700 °C synthesis temperature) loaded with 9,10-phenanthrenequinones, three-electrode set-up, free-standing mats.[87] Anjos *et al.*: nanodiamond-derived carbon onions (1800 °C synthesis temperature), three-electrode set-up, dropcast on glassy carbon.[139] Gu *et al.*: nanodiamond-derived carbon onions (1800 °C synthesis temperature) oxidized with H_2SO_4/HNO_3, two-electrode set-up, 1 M $LiPF_6$ in PC, PTFE-bound electrodes (10 mass%).[124] Liu *et al.*: nanodiamond-derived carbon onions (1650 °C synthesis temperature with further oxidation in air at 400 °C) electrochemically oxidized in 1 M H_2SO_4, three-electrode set-up, dropcast on glassy carbon.[140]

mechanisms responsible for the enhanced electrochemical performance of the PANI-nanodiamond composite (at least at low scan rates). A larger surface area in contact with the electrolyte is a direct result of the nanoscopic size of carbon onions, nanodiamonds, and nanodiamond soot particles and the change in the surface morphology of the PANI (increased roughness) that can be seen with electron microscopy (Fig. 11F). The best enhancement was found when using nanodiamond-containing raw detonation soot. Apparently, this material, which is a mixture of carbon onions, nanodiamonds, amorphous carbon, and other carbon nanoforms, provides an optimal combination of mechanical strength (nanodiamonds),

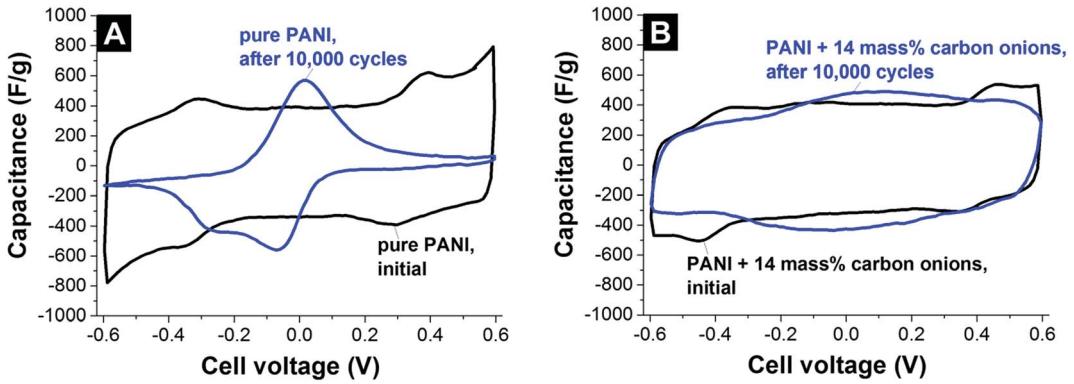

Fig. 15 Cyclic voltammograms of nanodiamond-derived carbon onions (1800 °C synthesis temperature) coated with PANI. Electrodes are PTFE-bound (3 mass%) and measured in a two-electrode configuration using 1 M H_2SO_4 recorded at a scan rate of 1 mV s^{-1}. (A) Pure PANI electrodes. (B) Carbon onion/PANI composite with 14 mass% carbon onions. Data adapted from ref. 132.

conductivity (carbon onions, graphitic carbon), and surface roughness (all together).[132]

Plonska-Brzezinska *et al.* used an *in situ* polymerization technique by first functionalizing nanodiamond-derived carbon onions with *p*-phenylenediamine or 4-aminobenzoic acid and subsequent growth of PANI on the surface groups using the synthesis method from ref. 149 and 150. The functionalized carbon onions were soluble in polar solvents and an increased hydrophilicity and wettability was achieved in aqueous electrolytes.[74] The capacitance measured in 0.1 M H_2SO_4 at 5 mV s^{-1} was 353 F g^{-1} for pure PANI, 207 F g^{-1} for the carbon onion/PANI hybrid with 4-amino-benzoic acid (4-ABAc) and carbon onions, and 155 F g^{-1} for the hybrid with poly-*p*-PDA and carbon onions. These values were slightly smaller than those reported in ref. 132, maybe due to the lower molarity of the electrolyte.

Another well-known inexpensive electroactive polymer is polypyrrole (Ppy) with comparable high conductivity and high stability in aqueous electrolytes. In the study by Mykhailiv *et al.*, carbon onion/polypyrrole hybrids were prepared by chemical polymerization of pyrrole.[138] Carbon onions and sodium dodecyl sulfate (SDS) functionalized carbon onions were coated by Ppy using $FeCl_3$ and pyrrole (Fig. 12G). Negatively charged surface functional groups of carbon onions interact with the pyrrole monomers leading to nucleation centers for the polymerization of pyrrole.[138] The largest capacitance was 805 F g^{-1} in 0.1 M TBA-ClO_4 in ACN at 5 mV s^{-1} scan rate with cyclic voltammetry and smaller values were obtained at higher rates (384 F g^{-1} at 100 mV s^{-1}, *i.e.*, −52%). The capacitance value of 384 F g^{-1} is derived from integration of the cyclic voltammogram and therefore more representative than the values derived from the current at a specific potential in the CV (in this case: 805 F g^{-1} at 0.1 V *versus* Ag/AgCl). The strong decrease in capacitance with increasing scan rate can be attributed to the inaccessibility of parts of the electrode at higher rates or degradation phenomena. Degradation of the electrode is supported by the low stability after 500 cycles at 100 mV s^{-1} of ∼20% and ∼35% depending on the potential window of −1 V to +0.3 V and −2 V to +0.6 V, respectively.[138]

Like for PANI and PPy, carbon onions can also be used as conductive substrates for poly(3,4-ethylenedioxythiophene):poly(styrenesulfonate) (PEDOT:PSS). Plonska-Brzezinska *et al.* used nanodiamond-derived carbon onions as well as their acid-oxidized form for coating with PEDOT:PSS layers.[73] By increasing the amount of PEDOT:PSS in the composite a maximum capacitance of 95 F g^{-1} was reached (1 : 1 mass ratio) for the composite with neat carbon onions and 47 F g^{-1} for the composite with oxidized carbon onions.[73]

5. Conclusions

This work provides an overview of electrochemical applications of carbon onions, and especially of nanodiamond-derived carbon onions. Several synthesis methods exist, but a standard method, with a high yield, reproducibility, and full control of structure, is the annealing of detonation nanodiamond powders. According to the synthesis conditions several properties, such as surface area and conductivity, can be tuned. Carbon onions as supercapacitor electrode materials present a superior rate handling behavior but suffer from a comparatively low specific energy. To overcome this issue, composites with metal oxides, conducting polymers, other redox species, as well as creation of surface functional groups can be used to induce the redox activity of carbon onions.

Carbon onions present a nearly ideal substrate for coating with redox-active substances due to their external and fully accessible surface area, combined with a high degree of sp^2-hybridized carbon ordering. In addition, carbon onions can be used as a potent conductive additive which enhances the power handling ability of supercapacitor carbon electrodes more than conventional carbon black or graphite nanoparticles. Further research aimed at enhancing the surface area of carbon onions and improving the rate handling for advanced redox-active hybrid electrodes will help to further promote the use of this unique carbon nanomaterial for electrochemical applications.

Acknowledgements

The authors thank Prof. Eduard Arzt (INM) for his continuing support. We acknowledge funding from the German Federal Ministry for Research and Education (BMBF) in support of the nanoEES^{3D} project (award number 03EK3013) as part of the strategic funding initiative energy storage framework. This work was supported by the CREATe-Network Project, Horizon 2020 of the European Commission (RISE Project No. 644013). The authors thank Prof. Gleb Yushin (Georgia Tech) for supporting us with experimental data and useful discussions.

References

1 A. H. C. Neto, The carbon new age, *Mater. Today*, 2010, **13**(3), 12–17.
2 J. Bartelmess and S. Giordani, Carbon nano-onions (multilayer fullerenes): chemistry and applications, *Beilstein J. Nanotechnol.*, 2014, **5**(1), 1980–1998.
3 M. G. Crestani, I. Puente-Lee, L. Rendón-Vazquez, P. Santiago, F. del Rio, D. Morales-Morales, *et al.*, The catalytic reduction of carbon dioxide to carbon onion particles by platinum catalysts, *Carbon*, 2005, **43**(12), 2621–2624.
4 C. Portet, G. Yushin and Y. Gogotsi, Electrochemical performance of carbon onions, nanodiamonds, carbon black and multiwalled nanotubes in electrical double layer capacitors, *Carbon*, 2007, **45**(13), 2511–2518.
5 S. Porada, L. Borchardt, M. Oschatz, M. Bryjak, J. Atchison, K. Keesman, *et al.*, Direct prediction of the desalination performance of porous carbon electrodes for capacitive deionization, *Energy Environ. Sci.*, 2013, **6**(12), 3700–3712.
6 D. Pech, M. Brunet, H. Durou, P. Huang, V. Mochalin, Y. Gogotsi, *et al.*, Ultrahigh-power micrometre-sized supercapacitors based on onion-like carbon, *Nat. Nanotechnol.*, 2010, **5**(9), 651–654.
7 N. Jäckel, D. Weingarth, M. Zeiger, M. Aslan, I. Grobelsek and V. Presser, Comparison of carbon onions and carbon

blacks as conductive additives for carbon supercapacitors in organic electrolytes, *J. Power Sources*, 2014, **272**, 1122–1133.

8 J. K. McDonough and Y. Gogotsi, Carbon onions: synthesis and electrochemical applications, *Electrochem. Soc. Interface*, 2013, **22**(3), 61–65.

9 M. E. Plonska-Brzezinska and L. Echegoyen, Carbon nano-onions for supercapacitor electrodes: recent developments and applications, *J. Mater. Chem. A*, 2013, **1**(44), 13703–13714.

10 Z. Yang, J. Zhang, M. C. Kintner-Meyer, X. Lu, D. Choi, J. P. Lemmon, *et al.*, Electrochemical energy storage for green grid, *Chem. Rev.*, 2011, **111**(5), 3577–3613.

11 J. R. Miller, Valuing reversible energy storage, *Science*, 2012, **335**(6074), 1312–1313.

12 D. Dubal, O. Ayyad, V. Ruiz and P. Gómez-Romero, Hybrid energy storage: the merging of battery and supercapacitor chemistries, *Chem. Soc. Rev.*, 2015, **44**(7), 1777–1790.

13 F. X. Index, *Nanocarbons for Advanced Energy Storage*, Wiley-VCH Verlag GmbH & Co. KGaA, 2015, p. 455–464.

14 F. Béguin, V. Presser, A. Balducci and E. Frackowiak, Carbons and Electrolytes for Advanced Supercapacitors, *Adv. Mater.*, 2014, **26**(14), 2219–2251.

15 A. Manthiram, S. H. Chung and C. Zu, Lithium–Sulfur Batteries: Progress and Prospects, *Adv. Mater.*, 2015, **27**(12), 1980–2006.

16 S. Goriparti, E. Miele, F. de Angelis, E. Di Fabrizio, R. P. Zaccaria and C. Capiglia, Review on recent progress of nanostructured anode materials for Li-ion batteries, *J. Power Sources*, 2014, **257**, 421–443.

17 A. Laheäär, P. Przygocki, Q. Abbas and F. Béguin, Appropriate methods for evaluating the efficiency and capacitive behavior of different types of supercapacitors, *Electrochem. Commun.*, 2015, **60**, 21–25.

18 P. Simon, Y. Gogotsi and B. Dunn, Where Do Batteries End and Supercapacitors Begin?, *Science*, 2014, **343**, 1210–1211.

19 J. R. Miller and A. F. Burke, Electrochemical capacitors: challenges and opportunities for real-world applications, *Electrochem. Soc. Interface*, 2008, **17**(1), 53.

20 T. A. Centeno, O. Sereda and F. Stoeckli, Capacitance in carbon pores of 0.7 to 15 nm: a regular pattern, *Phys. Chem. Chem. Phys.*, 2011, **13**(27), 12403–12406.

21 P. Bandaru, H. Yamada, R. Narayanan and M. Hoefer, Charge transfer and storage in nanostructures, *Mater. Sci. Eng., R*, 2015, **96**, 1–69.

22 B. Akinwolemiwa, C. Peng and G. Z. Chen, Redox electrolytes in supercapacitors, *J. Electrochem. Soc.*, 2015, **162**(5), A5140–A5147.

23 I. Hadjipaschalis, A. Poullikkas and V. Efthimiou, Overview of current and future energy storage technologies for electric power applications, *Renewable Sustainable Energy Rev.*, 2009, **13**(6–7), 1513–1522.

24 Y. Zhang, H. Feng, X. B. Wu, L. Z. Wang, A. Q. Zhang, T. C. Xia, *et al.*, Progress of electrochemical capacitor electrode materials: a review, *Int. J. Hydrogen Energy*, 2009, **34**(11), 4889–4899.

25 M. Vangari, T. Pryor and L. Jiang, Supercapacitors: Review of Materials and Fabrication Methods, *J. Energy Eng.*, 2013, **139**(2), 72–79.

26 R. Borgohain, J. Li, J. P. Selegue and Y.-T. Cheng, Electrochemical study of functionalized carbon nano-onions for high-performance supercapacitor electrodes, *J. Phys. Chem. C*, 2012, **116**(28), 15068–15075.

27 M. E. Plonska-Brzezinska, D. M. Brus, A. Molina-Ontoria and L. Echegoyen, Synthesis of carbon nano-onion and nickel hydroxide/oxide composites as supercapacitor electrodes, *RSC Adv.*, 2013, **3**(48), 25891–25901.

28 W. Gu and G. Yushin, Review of nanostructured carbon materials for electrochemical capacitor applications: advantages and limitations of activated carbon, carbide-derived carbon, zeolite-templated carbon, carbon aerogels, carbon nanotubes, onion-like carbon, and graphene, *Wiley Interdiscip. Rev.: Energy Environ.*, 2014, **3**(5), 424–473.

29 I. Suarez-Martinez, N. Grobert and C. P. Ewels, Nomenclature of sp^2 carbon nanoforms, *Carbon*, 2012, **50**(3), 741–747.

30 D. Ugarte, Curling and closure of graphitic networks under electron-beam irradiation, *Nature*, 1992, **359**(6397), 707–709.

31 S. Iijima, Direct observation of the tetrahedral bonding in graphitized carbon black by high resolution electron microscopy, *J. Cryst. Growth*, 1980, **50**(3), 675–683.

32 M. Zeiger, N. Jäckel, M. Aslan, D. Weingarth and V. Presser, Understanding structure and porosity of nanodiamond-derived carbon onions, *Carbon*, 2015, **84**, 584–598.

33 A. Bianco, H.-M. Cheng, T. Enoki, Y. Gogotsi, R. H. Hurt, N. Koratkar, *et al.*, All in the graphene family – a recommended nomenclature for two-dimensional carbon materials, *Carbon*, 2013, **65**, 1–6.

34 O. A. Shenderova and D. M. Gruen, *Ultrananocrystalline diamond: synthesis, properties and applications*, William Andrew, 2012.

35 B. Maquin, A. Derré, C. Labrugère, M. Trinquecoste, P. Chadeyron and P. Delhaès, Submicronic powders containing carbon, boron and nitrogen: their preparation by chemical vapour deposition and their characterization, *Carbon*, 2000, **38**(1), 145–156.

36 V. Serin, R. Brydson, A. Scott, Y. Kihn, O. Abidate, B. Maquin, *et al.*, Evidence for the solubility of boron in graphite by electron energy loss spectroscopy, *Carbon*, 2000, **38**(4), 547–554.

37 C. He, N. Zhao, C. Shi, X. Du and J. Li, Carbon nanotubes and onions from methane decomposition using Ni/Al catalysts, *Mater. Chem. Phys.*, 2006, **97**(1), 109–115.

38 S. Tsai, C. Lee, C. Chao and H. Shih, A novel technique for the formation of carbon-encapsulated metal nanoparticles on silicon, *Carbon*, 2000, **38**(5), 781–785.

39 S.-S. Hou, D.-H. Chung and T.-H. Lin, High-yield synthesis of carbon nano-onions in counterflow diffusion flames, *Carbon*, 2009, **47**(4), 938–947.

40 M. Choucair and J. A. Stride, The gram-scale synthesis of carbon onions, *Carbon*, 2012, **50**(3), 1109–1115.

41 Y. Gao, Y. Zhou, J. Park, H. Wang, X. N. He, H. Luo, *et al.*, Resonant excitation of precursor molecules in improving the particle crystallinity, growth rate and optical limiting performance of carbon nano-onions, *Nanotechnology*, 2011, **22**(16), 165604.
42 M. Zhao, H. Song, X. Chen and W. Lian, Large-scale synthesis of onion-like carbon nanoparticles by carbonization of phenolic resin, *Acta Mater.*, 2007, **55**(18), 6144–6150.
43 M. Bystrzejewski, M. H. Rummeli, T. Gemming, H. Lange and A. Huczko, Catalyst-free synthesis of onion-like carbon nanoparticles, *New Carbon Mater.*, 2010, **25**(1), 1–8.
44 D.-H. Chung, T.-H. Lin and S.-S. Hou, Flame synthesis of carbon nano-onions enhanced by acoustic modulation, *Nanotechnology*, 2010, **21**(43), 435604.
45 M. Choi, I. S. Altman, Y. J. Kim, P. V. Pikhitsa, S. Lee, G. S. Park, *et al.*, Formation of Shell-Shaped Carbon Nanoparticles Above a Critical Laser Power in Irradiated Acetylene, *Adv. Mater.*, 2004, **16**(19), 1721–1725.
46 J. Huang, H. Yasuda and H. Mori, Highly curved carbon nanostructures produced by ball-milling, *Chem. Phys. Lett.*, 1999, **303**(1), 130–134.
47 X. H. Chen, H. S. Yang, G. T. Wu, M. Wang, F. M. Deng, X. B. Zhang, *et al.*, Generation of curved or closed-shell carbon nanostructures by ball-milling of graphite, *J. Cryst. Growth*, 2000, **218**(1), 57–61.
48 T. Cabioc'h, M. Jaouen, E. Thune, P. Guerin, C. Fayoux and M. Denanot, Carbon onions formation by high-dose carbon ion implantation into copper and silver, *Surf. Coat. Technol.*, 2000, **128**, 43–50.
49 E. Thune, T. Cabioc'h, P. Guérin, M.-F. Denanot and M. Jaouen, Nucleation and growth of carbon onions synthesized by ion-implantation: a transmission electron microscopy study, *Mater. Lett.*, 2002, **54**(2), 222–228.
50 H. Lange, M. Sioda, A. Huczko, Y. Zhu, H. Kroto and D. Walton, Nanocarbon production by arc discharge in water, *Carbon*, 2003, **41**(8), 1617–1623.
51 M. Ishigami, J. Cumings, A. Zettl and S. Chen, A simple method for the continuous production of carbon nanotubes, *Chem. Phys. Lett.*, 2000, **319**(5), 457–459.
52 N. Sano, H. Wang, M. Chhowalla, I. Alexandrou and G. Amaratunga, Nanotechnology: synthesis of carbon 'onions' in water, *Nature*, 2001, **414**(6863), 506–507.
53 W. Lian, H. Song, X. Chen, L. Li, J. Huo, M. Zhao, *et al.*, The transformation of acetylene black into onion-like hollow carbon nanoparticles at 1000 °C using an iron catalyst, *Carbon*, 2008, **46**(3), 525–530.
54 J.-C. Fan, H.-H. Sung, C.-R. Lin and M.-H. Lai, The production of onion-like carbon nanoparticles by heating carbon in a liquid alcohol, *J. Mater. Chem.*, 2012, **22**(19), 9794.
55 S. Tomita, A. Burian, J. C. Dore, D. LeBolloch, M. Fujii and S. Hayashi, Diamond nanoparticles to carbon onions transformation: X-ray diffraction studies, *Carbon*, 2002, **40**(9), 1469–1474.
56 Y. V. Butenko, V. L. Kuznetsov, A. L. Chuvilin, V. N. Kolomiichuk, S. V. Stankus, R. A. Khairulin, *et al.*, Kinetics of the graphitization of dispersed diamonds at "low" temperatures, *J. Appl. Phys.*, 2000, **88**(7), 4380.
57 S. Tomita, T. Sakurai, H. Ohta, M. Fujii and S. Hayashi, Structure and electronic properties of carbon onions, *J. Chem. Phys.*, 2001, **114**(17), 7477.
58 O. O. Mykhaylyk, Y. M. Solonin, D. N. Batchelder and R. Brydson, Transformation of nanodiamond into carbon onions: a comparative study by high-resolution transmission electron microscopy, electron energy-loss spectroscopy, X-ray diffraction, small-angle X-ray scattering, and ultraviolet Raman spectroscopy, *J. Appl. Phys.*, 2005, **97**(7), 074302–074316.
59 Y. V. Butenko, V. L. Kuznetsov, E. A. Paukshtis, A. I. Stadnichenko, I. N. Mazov, S. I. Moseenkov, *et al.*, The Thermal Stability of Nanodiamond Surface Groups and Onset of Nanodiamond Graphitization, *Fullerenes, Nanotubes, Carbon Nanostruct.*, 2006, **14**(2–3), 557–564.
60 Q. Zou, Y. G. Li, B. Lv, M. Z. Wang, L. H. Zou and Y. C. Zhao, Transformation of onion-like carbon from nanodiamond by annealing, *Inorg. Mater.*, 2010, **46**(2), 127–131.
61 V. L. Kuznetsov, A. L. Chuvilin, Y. V. Butenko, I. Y. Mal'kov and V. M. Titov, Onion-like carbon from ultra-disperse diamond, *Chem. Phys. Lett.*, 1994, **222**(4), 343–348.
62 N. Xu, J. Chen and S. Deng, Effect of heat treatment on the properties of nano-diamond under oxygen and argon ambient, *Diamond Relat. Mater.*, 2002, **11**(2), 249–256.
63 A. Aleksenskii, M. Baidakova, A. Y. Vul, V. Y. Davydov and Y. A. Pevtsova, Diamond–graphite phase transition in ultradisperse-diamond clusters, *Phys. Solid State*, 1997, **39**(6), 1007–1015.
64 M. Baidakova, V. Siklitsky and A. Y. Vul, Ultradisperse-diamond nanoclusters. Fractal structure and diamond–graphite phase transition, *Chaos, Solitons Fractals*, 1999, **10**(12), 2153–2163.
65 D. Weingarth, M. Zeiger, N. Jäckel, M. Aslan, G. Feng and V. Presser, Graphitization as a universal tool to tailor the potential-dependent capacitance of carbon supercapacitors, *Adv. Energy Mater.*, 2014, **4**, 1400316.
66 O. E. Andersson, B. Prasad, H. Sato, T. Enoki, Y. Hishiyama, Y. Kaburagi, *et al.*, Structure and electronic properties of graphite nanoparticles, *Phys. Rev. B: Condens. Matter Mater. Phys.*, 1998, **58**(24), 16387.
67 J. Chen, S. Deng, J. Chen, Z. Yu and N. Xu, Graphitization of nanodiamond powder annealed in argon ambient, *Appl. Phys. Lett.*, 1999, **74**(24), 3651–3653.
68 F. Y. Xie, W. G. Xie, L. Gong, W. H. Zhang, S. H. Chen, Q. Z. Zhang, *et al.*, Surface characterization on graphitization of nanodiamond powder annealed in nitrogen ambient, *Surf. Interface Anal.*, 2010, **42**(9), 1514–1518.
69 A. Aleksenskii, M. Baidakova, A. Y. Vul, A. Dideikin and V. Siklitskii, Effect of hydrogen on the structure of ultradisperse diamond, *Phys. Solid State*, 2000, **42**(8), 1575–1578.
70 O. Mykhailiv, A. Lapinski, A. Molina-Ontoria, E. Regulska, L. Echegoyen, A. T. Dubis, *et al.*, Influence of the Synthetic Conditions on the Structural and

Electrochemical Properties of Carbon Nano-Onions, *ChemPhysChem*, 2015, **16**(10), 2182–2191.

71 M. E. Plonska-Brzezinska, A. T. Dubis, A. Lapinski, A. Villalta-Cerdas and L. Echegoyen, Electrochemical propertiesof oxidized carbon nano-onions: DRIFTS-FTIR and Raman spectroscopic analyses, *ChemPhysChem*, 2011, **12**(14), 2659–2668.

72 M. E. Plonska-Brzezinska, A. Lapinski, A. Z. Wilczewska, A. T. Dubis, A. Villalta-Cerdas, K. Winkler, *et al.*, The synthesis and characterization of carbon nano-onions produced by solution ozonolysis, *Carbon*, 2011, **49**(15), 5079–5089.

73 M. E. Plonska-Brzezinska, M. Lewandowski, M. Błaszyk, A. Molina-Ontoria, T. Luciński and L. Echegoyen, Preparation and Characterization of Carbon Nano-Onion/PEDOT: PSS Composites, *ChemPhysChem*, 2012, **13**(18), 4134–4141.

74 M. E. Plonska-Brzezinska, J. Mazurczyk, B. Palys, J. Breczko, A. Lapinski, A. T. Dubis, *et al.*, Preparation and Characterization of Composites that Contain Small Carbon Nano-Onions and Conducting Polyaniline, *Chem.–Eur. J.*, 2012, **18**(9), 2600–2608.

75 M. E. Plonska-Brzezinska, A. Molina-Ontoria and L. Echegoyen, Post-modification by low-temperature annealing of carbon nano-onions in the presence of carbohydrates, *Carbon*, 2014, **67**, 304–317.

76 A. V. Gubarevich, J. Kitamura, S. Usuba, H. Yokoi, Y. Kakudate and O. Odawara, Onion-like carbon deposition by plasma spraying of nanodiamonds, *Carbon*, 2003, **41**(13), 2601–2606.

77 J. Xiao, G. Ouyang, P. Liu, C. Wang and G. Yang, Reversible nanodiamond-carbon onion phase transformations, *Nano Lett.*, 2014, **14**(6), 3645–3652.

78 F. Banhart, T. Füller, P. Redlich and P. Ajayan, The formation, annealing and self-compression of carbon onions under electron irradiation, *Chem. Phys. Lett.*, 1997, **269**(3), 349–355.

79 D. Ugarte, Morphology and structure of graphitic soot particles generated in arc-discharge C_{60} production, *Chem. Phys. Lett.*, 1992, **198**(6), 596–602.

80 A. B. Du, X. G. Liu, D. J. Fu, P. D. Han and B. S. Xu, Onion-like fullerenes synthesis from coal, *Fuel*, 2007, **86**(1–2), 294–298.

81 Y. Gao, Y. S. Zhou, M. Qian, X. N. He, J. Redepenning, P. Goodman, *et al.*, Chemical activation of carbon nano-onions for high-rate supercapacitor electrodes, *Carbon*, 2013, **51**, 52–58.

82 R. Borgohain, J. Yang, J. P. Selegue and D. Y. Kim, Controlled synthesis, efficient purification, and electrochemical characterization of arc-discharge carbon nano-onions, *Carbon*, 2014, **66**, 272–284.

83 J. K. McDonough, A. I. Frolov, V. Presser, J. Niu, C. H. Miller, T. Ubieto, *et al.*, Influence of the structure of carbon onions on their electrochemical performance in supercapacitor electrodes, *Carbon*, 2012, **50**(9), 3298–3309.

84 E. G. Bushueva, P. S. Galkin, A. V. Okotrub, L. G. Bulusheva, N. N. Gavrilov, V. L. Kuznetsov, *et al.*, Double layer supercapacitor properties of onion-like carbon materials, *Phys. Status Solidi B*, 2008, **245**(10), 2296–2299.

85 M. E. Plonska-Brzezinska, A. Palkar, K. Winkler and L. Echegoyen, Electrochemical properties of small carbon nano-onion films, *Electrochem. Solid-State Lett.*, 2010, **13**(4), K35–K8.

86 M. V. K. Azhagan, M. V. Vaishampayan and M. V. Shelke, Synthesis and electrochemistry of pseudocapacitive multilayer fullerenes and MnO_2 nanocomposites, *J. Mater. Chem. A*, 2014, **2**(7), 2152–2159.

87 M. Zeiger, N. Jäckel, D. Weingarth and V. Presser, Vacuum or flowing argon: What is the best synthesis atmosphere for nanodiamond-derived carbon onions for supercapacitor electrodes?, *Carbon*, 2015, **94**, 507–517.

88 V. N. Mochalin, O. Shenderova, D. Ho and Y. Gogotsi, The properties and applications of nanodiamonds, *Nat. Nanotechnol.*, 2012, **7**(1), 11–23.

89 D. P. Mitev, A. T. Townsend, B. Paull and P. N. Nesterenko, Direct sector field ICP-MS determination of metal impurities in detonation nanodiamond, *Carbon*, 2013, **60**, 326–334.

90 X. Fang, J. Mao, E. Levin and K. Schmidt-Rohr, Nonaromatic Core–Shell Structure of Nanodiamond from Solid-State NMR Spectroscopy, *J. Am. Chem. Soc.*, 2009, **131**(4), 1426–1435.

91 A. Panich, A. Shames, H.-M. Vieth, E. Ōsawa, M. Takahashi and A. Y. Vul, Nuclear magnetic resonance study of ultrananocrystalline diamonds, *Eur. Phys. J. B*, 2006, **52**(3), 397–402.

92 M. Dubois, K. Guérin, E. Petit, N. Batisse, A. Hamwi, N. Komatsu, *et al.*, Solid-state NMR study of nanodiamonds produced by the detonation technique, *J. Phys. Chem. C*, 2009, **113**(24), 10371–10378.

93 A. Krüger, F. Kataoka, M. Ozawa, T. Fujino, Y. Suzuki, A. Aleksenskii, *et al.*, Unusually tight aggregation in detonation nanodiamond: identification and disintegration, *Carbon*, 2005, **43**(8), 1722–1730.

94 V. Kuznetsov and Y. V. Butenko, Synthesis and properties of nanostructured carbon materials: nanodiamond, onion-like carbon and carbon nanotubes, *Nanostructured Materials and Coatings for Biomedical and Sensor Applications*, Springer, 2003, pp. 187–202.

95 F. Cataldo and A. P. Koscheev, A study on the action of ozone and on the thermal stability of nanodiamond, *Fullerenes, Nanotubes, Carbon Nanostruct.*, 2003, **11**(3), 201–218.

96 B. J. M. Etzold, I. Neitzel, M. Kett, F. Strobl, V. N. Mochalin and Y. Gogotsi, Layer-by-Layer Oxidation for Decreasing the Size of Detonation Nanodiamond, *Chem. Mater.*, 2014, **26**(11), 3479–3484.

97 P. Ganesh, P. Kent and V. Mochalin, Formation, characterization, and dynamics of onion-like carbon structures for electrical energy storage from nanodiamonds using reactive force fields, *J. Appl. Phys.*, 2011, **110**(7), 073506.

98 T. Jiang and K. Xu, FTIR study of ultradispersed diamond powder synthesized by explosive detonation, *Carbon*, 1995, **33**(12), 1663–1671.

99 B. Spitsyn, M. Gradoboev, T. Galushko, T. Karpukhina, N. Serebryakova and I. Kulakova, *et al.*, Purification and functionalization of nanodiamond, *Synthesis, properties and applications of ultrananocrystalline diamond*, Springer, 2005, pp. 241–52.

100 T. Petit, J.-C. Arnault, H. A. Girard, M. Sennour and P. Bergonzo, Early stages of surface graphitization on nanodiamond probed by X-ray photoelectron spectroscopy, *Phys. Rev. B: Condens. Matter Mater. Phys.*, 2011, **84**(23), 233407.

101 K. Bogdanov, A. Fedorov, V. Osipov, T. Enoki, K. Takai, T. Hayashi, *et al.*, Annealing-induced structural changes of carbon onions: high-resolution transmission electron microscopy and Raman studies, *Carbon*, 2014, **73**, 78–86.

102 A. Ferrari, A. Libassi, B. Tanner, V. Stolojan, J. Yuan, L. Brown, *et al.*, Density, sp^3 fraction, and cross-sectional structure of amorphous carbon films determined by X-ray reflectivity and electron energy-loss spectroscopy, *Phys. Rev. B: Condens. Matter Mater. Phys.*, 2000, **62**(16), 11089.

103 J. Cebik, J. K. McDonough, F. Peerally, R. Medrano, I. Neitzel, Y. Gogotsi, *et al.*, Raman spectroscopy study of the nanodiamond-to-carbon onion transformation, *Nanotechnology*, 2013, **24**(20), 205703.

104 V. L. Kuznetsov, I. L. Zilberberg, Y. V. Butenko, A. L. Chuvilin and B. Segall, Theoretical study of the formation of closed curved graphite-like structures during annealing of diamond surface, *J. Appl. Phys.*, 1999, **86**(2), 863.

105 A. Siklitskaya, S. Yastrebov and R. Smith, Variable step radial ordering in carbon onions, *Diamond Relat. Mater.*, 2013, **32**, 32–35.

106 A. Siklitskaya, S. Yastrebov and R. Smith, Structure-induced negatively skewed X-ray diffraction pattern of carbon onions, *J. Appl. Phys.*, 2013, **114**(13), 134305.

107 M. Ozawa, H. Goto, M. Kusunoki and E. Ōsawa, Continuously Growing Spiral Carbon Nanoparticles as the Intermediates in the Formation of Fullerenes and Nanoonions, *J. Phys. Chem. B*, 2002, **106**(29), 7135–7138.

108 E. Akatyeva, J. Huang and T. Dumitrică, Edge-mediated dislocation processes in multishell carbon nano-onions?, *Phys. Rev. Lett.*, 2010, **105**(10), 106102.

109 Z. Qiao, J. Li, N. Zhao, C. Shi and P. Nash, Graphitization and microstructure transformation of nanodiamond to onion-like carbon, *Scr. Mater.*, 2006, **54**(2), 225–229.

110 L. Reinert, M. Zeiger, S. Suarez, V. Presser and F. Mücklich, Dispersion analysis of carbon nanotubes, carbon onions, and nanodiamonds for their application as reinforcement phase in nickel metal matrix composites, *RSC Adv.*, 2015, **5**, 95149–95159.

111 V. Kuznetsov, S. Moseenkov, A. Ischenko, A. Romanenko, T. Buryakov, O. Anikeeva, *et al.*, Controllable electromagnetic response of onion-like carbon based materials, *Phys. Status Solidi B*, 2008, **245**(10), 2051–2054.

112 Y. Gan and F. Banhart, The mobility of carbon atoms in graphitic nanoparticles studied by the relaxation of strain in carbon onions, *Adv. Mater.*, 2008, **20**(24), 4751–4754.

113 E. D. Obraztsova, M. Fujii, S. Hayashi, V. L. Kuznetsov, Y. V. Butenko and A. L. Chuvilin, Raman identification of onion-like carbon, *Carbon*, 1998, **36**(5–6), 821–826.

114 D. Roy, M. Chhowalla, H. Wang, N. Sano, I. Alexandrou, T. W. Clyne, *et al.*, Characterisation of carbon nano-onions using Raman spectroscopy, *Chem. Phys. Lett.*, 2003, **373**(1–2), 52–56.

115 S. N. Bokova-Sirosh, A. V. Pershina, V. L. Kuznetsov, A. V. Ishchenko, S. I. Moseenkov, A. S. Orekhov, *et al.*, Raman Spectra for Characterization of Onion-Like Carbon, *J. Nanoelectron. Optoelectron.*, 2013, **8**(1), 106–109.

116 F. Tuinstra, Raman Spectrum of Graphite, *J. Chem. Phys.*, 1970, **53**(3), 1126.

117 A. Ferrari and J. Robertson, Resonant Raman spectroscopy of disordered, amorphous, and diamondlike carbon, *Phys. Rev. B: Condens. Matter Mater. Phys.*, 2001, **64**(7), 075414.

118 V. V. Roddatis, V. L. Kuznetsov, Y. V. Butenko, D. S. Su and R. Schlögl, Transformation of diamond nanoparticles into carbon onions under electron irradiation, *Phys. Chem. Chem. Phys.*, 2002, **4**(10), 1964–1967.

119 L. Joly-Pottuz, N. Matsumoto, H. Kinoshita, B. Vacher, M. Belin, G. Montagnac, *et al.*, Diamond-derived carbon onions as lubricant additives, *Tribol. Int.*, 2008, **41**(2), 69–78.

120 V. Kuznetsov, Y. V. Butenko, A. Chuvilin, A. Romanenko and A. Okotrub, Electrical resistivity of graphitized ultra-disperse diamond and onion-like carbon, *Chem. Phys. Lett.*, 2001, **336**(5), 397–404.

121 Q. Zou, M. Wang, Y. Li, Y. Zhao and L. Zou, Fabrication of onion-like carbon from nanodiamond by annealing, *Sci. China, Ser. E: Technol. Sci.*, 2009, **52**(12), 3683–3689.

122 V. Kuznetsov, Y. V. Butenko, V. Zaikovskii and A. Chuvilin, Carbon redistribution processes in nanocarbons, *Carbon*, 2004, **42**(5), 1057–1061.

123 N. Sano, H. Wang, I. Alexandrou, M. Chhowalla, K. B. K. Teo, G. A. J. Amaratunga, *et al.*, Properties of carbon onions produced by an arc discharge in water, *J. Appl. Phys.*, 2002, **92**(5), 2783.

124 W. Gu, N. Peters and G. Yushin, Functionalized carbon onions, detonation nanodiamond and mesoporous carbon as cathodes in Li-ion electrochemical energy storage devices, *Carbon*, 2013, **53**, 292–301.

125 A. Krüger, F. Kataoka, M. Ozawa, T. Fujino, Y. Suzuki, A. E. Aleksenskii, *et al.*, Unusually tight aggregation in detonation nanodiamond: identification and disintegration, *Carbon*, 2005, **43**(8), 1722–1730.

126 A. Kornyshev, N. Luque and W. Schmickler, Differential capacitance of ionic liquid interface with graphite: the story of two double layers, *J. Solid State Electrochem.*, 2014, **18**(5), 1345–1349.

127 P. Ruch, R. Kötz and A. Wokaun, Electrochemical characterization of single-walled carbon nanotubes for electrochemical double layer capacitors using non-aqueous electrolyte, *Electrochim. Acta*, 2009, **54**(19), 4451–4458.

128 H. Gerischer, R. McIntyre, D. Scherson and W. Storck, Density of the electronic states of graphite: derivation

from differential capacitance measurements, *J. Phys. Chem.*, 1987, **91**(7), 1930–1935.

129 M. Zeiger, D. Weingarth and V. Presser, Quinone-Decorated Onion-Like Carbon/Carbon Fiber Hybrid Electrodes for High-Rate Supercapacitor Applications, *ChemElectroChem*, 2015, **2**(8), 1117–1127.

130 K. Jost, C. R. Perez, J. K. McDonough, V. Presser, M. Heon, G. Dion, *et al.*, Carbon coated textiles for flexible energy storage, *Energy Environ. Sci.*, 2011, **4**(12), 5060–5067.

131 P. F. Fulvio, R. T. Mayes, X. Wang, S. M. Mahurin, J. C. Bauer, V. Presser, *et al.*, "Brick-and-Mortar" Self-Assembly Approach to Graphitic Mesoporous Carbon Nanocomposites, *Adv. Funct. Mater.*, 2011, **21**(12), 2208–2215.

132 I. Kovalenko, D. G. Bucknall and G. Yushin, Detonation Nanodiamond and Onion-Like-Carbon-Embedded Polyaniline for Supercapacitors, *Adv. Funct. Mater.*, 2010, **20**(22), 3979–3986.

133 Y. Sun, Q. Wu, Y. Xu, H. Bai, C. Li and G. Shi, Highly conductive and flexible mesoporous graphitic films prepared by graphitizing the composites of graphene oxide and nanodiamond, *J. Mater. Chem.*, 2011, **21**(20), 7154.

134 J. M. Miller, *Ultracapacitor applications*, The Institution of Engineering and Technology, 2011.

135 K. Makgopa, P. M. Ejikeme, C. J. Jafta, K. Raju, M. Zeiger, V. Presser, *et al.*, A high-rate aqueous symmetric pseudocapacitor based on highly graphitized onion-like carbon/birnessite-type manganese oxide nanohybrids, *J. Mater. Chem. A*, 2015, **3**(7), 3480–3490.

136 R. Borgohain, J. P. Selegue and Y.-T. Cheng, Ternary composites of delaminated-MnO_2/PDDA/functionalized-CNOs for high-capacity supercapacitor electrodes, *J. Mater. Chem. A*, 2014, **2**(47), 20367–20373.

137 Y. Wang, S. F. Yu, C. Y. Sun, T. J. Zhu and H. Y. Yang, MnO_2/onion-like carbon nanocomposites for pseudocapacitors, *J. Mater. Chem.*, 2012, **22**(34), 17584–17588.

138 O. Mykhailiv, M. Imierska, M. Petelczyc, L. Echegoyen and M. E. Plonska-Brzezinska, Chemical *versus* Electrochemical Synthesis of Carbon Nano-onion/Polypyrrole Composites for Supercapacitor Electrodes, *Chem.–Eur. J.*, 2015, **21**(15), 5783–5793.

139 D. M. Anjos, J. K. McDonough, E. Perre, G. M. Brown, S. H. Overbury, Y. Gogotsi, *et al.*, Pseudocapacitance and performance stability of quinone-coated carbon onions, *Nano Energy*, 2013, **2**(5), 702–712.

140 Y. Liu and D. Y. Kim, Enhancement of Capacitance by Electrochemical Oxidation of Nanodiamond Derived Carbon Nano-Onions, *Electrochim. Acta*, 2014, **139**, 82–87.

141 F.-D. Han, B. Yao and Y.-J. Bai, Preparation of Carbon Nano-Onions and Their Application as Anode Materials for Rechargeable Lithium-Ion Batteries, *J. Phys. Chem. C*, 2011, **115**(18), 8923–8927.

142 Y. Wang, Z. J. Han, S. F. Yu, R. R. Song, H. H. Song, K. K. Ostrikov, *et al.*, Core-leaf onion-like carbon/MnO_2 hybrid nano-urchins for rechargeable lithium-ion batteries, *Carbon*, 2013, **64**, 230–236.

143 Y. Wang, G. Xing, Z. J. Han, Y. Shi, J. I. Wong, Z. X. Huang, *et al.*, Pre-lithiation of onion-like carbon/MoS_2 nano-urchin anodes for high-performance rechargeable lithium ion batteries, *Nanoscale*, 2014, **6**(15), 8884–8890.

144 E. Raymundo-Pinero, K. Kierzek, J. Machnikowski and F. Béguin, Relationship between the nanoporous texture of activated carbons and their capacitance properties in different electrolytes, *Carbon*, 2006, **44**(12), 2498–2507.

145 S. Roldán, C. Blanco, M. Granda, R. Menéndez and R. Santamaría, Towards a Further Generation of High-Energy Carbon-Based Capacitors by Using Redox-Active Electrolytes, *Angew. Chem., Int. Ed.*, 2011, **50**(7), 1699–1701.

146 S. M. Chathoth, D. M. Anjos, E. Mamontov, G. M. Brown and S. H. Overbury, Dynamics of phenanthrenequinone on carbon nano-onion surfaces probed by quasielastic neutron scattering, *J. Phys. Chem. B*, 2012, **116**(24), 7291–7295.

147 A. le Comte, D. Chhin, A. Gagnon, R. Retoux, T. Brousse and D. Belanger, Spontaneous grafting of 9,10-phenanthrenequinone on porous carbon as active electrode material in electrochemical capacitor in alkaline electrolyte, *J. Mater. Chem. A*, 2015, **3**(11), 6146–6156.

148 F. A. Armstrong, R. Camba, H. A. Heering, J. Hirst, L. J. Jeuken, A. K. Jones, *et al.*, Fast voltammetric studies of the kinetics and energetics of coupled electron-transfer reactions in proteins, *Faraday Discuss.*, 2000, **116**, 191–203.

149 F. Yılmaz and Z. Küçükyavuz, Conducting polymer composites of multiwalled carbon nanotube filled doped polyaniline, *J. Appl. Polym. Sci.*, 2009, **111**(2), 680–684.

150 H. Zengin, W. Zhou, J. Jin, R. Czerw, D. W. Smith, L. Echegoyen, *et al.*, Carbon nanotube doped polyaniline, *Adv. Mater.*, 2002, **14**(20), 1480–1483.

